1 *Type of the Paper: **Article***

2 **Study on Riparian Shading Envelope for Wetlands to Create Desirable Urban**
3 **Bioclimates**

4

5 **Abu Taib Mohammed Shahjahan [1]*, Khandaker Shabbir Ahmed [2] and Ismail Bin Said[3,]**

6 [1] Department of Architecture, American International University-Bangladesh (AIUB), 408/1 (new), Kuril,
7   Kuratoli Road, Dhaka-1229, Bangladesh; shahjahan0275@gmail.com
8 [2] Department of Architecture, Bangladesh University of Engineering and Technology, Dhaka 1000,
9   Bangladesh.; shabbir@arch.buet.ac.bd
10 [3] Department of Landscape Architecture, Faculty of Built Environment and Surveying, Universiti
11   Teknologi Malaysia, 81310 Skudai, Johor, Malaysia; ismailbinsaid@gmail.com
12 * Correspondence: Abu Taib Mohammed Shahjahan; shahjahan0275@gmail.com; Tel.: 008801730436953

13 **Abstract:** Climate change and rapid urbanization are adversely affecting the urban environment by
14 exacerbating the widely reported Urban Heat Island effect in Dhaka, Bangladesh. Two wetland areas with
15 variable riparian shadings in the warm-humid conditions of urban Dhaka had been investigated through field
16 campaigns on microclimatic parameters for their cooling potential on the surrounding urban fabric. It was
17 observed that an inversion layer of fully saturated air develops over the water surface of wetland, suppressing
18 evaporation from the wetland water surface layer, which was effectively reducing the heat exchange between
19 the water surface and the air layer above it through its action as an insulating vapor blanket. Because of this
20 effect, the wetland was unable to render as a source of coolth for the surrounding overheated urban area. This
21 effect of the inversion layer was more pronounced in the urban wetland without riparian shading either by urban
22 form or tree canopy. A Multiphysics simulation study conducted on the selected urban wetlands indicates the
23 effect of differential shading pattern on the relation between fetch and inversion layer thickness. This research
24 hypothesizes that the wetland can act as an urban adaption measure against the urban heat island effect by
25 potentially transforming them into Urban Cooling Island (UCI) towards a favorable urban bioclimate.

26 **Keywords:** urban bioclimate; urban cooling; urban wetland; riparian shading; inversion layer
27

28 **1.   Introduction**

29   Urbanization in the developing world is dramatic if compared with the standard of today's urbanized
30 world. Within a short period, the urban population in the developing world superseded the developed world.
31 However, most of the rural-urban migration in the developing world is for economic reasons, as the city offers
32 better opportunities in terms of livelihood. Still, in recent times, most of the rural-urban migrations in the
33 developing world are related to global climate change. Much of the urban areas of the developing world are in
34 the tropical zone, where urbanization is distinctive from climate, demography, and cultural point of view.
35 According to the IPCC, Bangladesh is the sixth most vulnerable country to climate change (IPCC, 2014). At
36 present, Dhaka is the densest and one of the most populated cities in the whole world; in 2016, its population
37 was more than 14 million [Ahmed 1993; BBS, 2016]. Wetlands and green spaces are diminishing due to
38 unprecedented and often unplanned urbanization, in addition to pressure from the housing sector. Within 20
39 years (1989-2009), urban wetlands in Dhaka metropolitan area have been reduced from 26.68% of the total city
40 area to 9.27%, which is approximately a 65% reduction [Ahmed *et al.*, 2013]. One of the climate-related
41 extreme that we are facing in Dhaka, like other megacities in the world, is Urban Heat Island (UHI), which is
42 exacerbated by growing global temperatures. From numerous studies on UHI mitigation, it can concur that

43 urban water bodies can play an active role in mitigating UHI through microclimatic cooling of the urban area
44 by creating cool spots. As these cool spots can transport coolth inside the urban fabric, they can be termed as
45 Urban Cooling Islands (UCIs). Besides the wetland, urban parks can also act as UCIs for their
46 evapotranspiration effect and shading of the trees. However, as the heat content capacity of the water is high, it
47 could counteract the UCIs effect if kept unshaded. Urban wetland Shaded by Buildings, topography, and shade
48 trees can have a proficient effect on microclimatic cooling. In contrast, riparian shade can have a positive effect
49 on the UCIs as well as on the water quality. The result of riparian shade on the water body is mostly observed
50 on the linear and narrow streams having a less urban build up on either side (Sun *et al.*, 2012). There are few
51 studies about the effect of riparian shade in the broader water body. Also, most of the studies suggest a small
52 area and regular (Euclidean shape) shape water body distributed at regular intervals in an urban area makes for
53 better Urban Cooling Island (UCIs) intensity. Hence, the primary research question is, how can the introduction
54 of riparian shade moderate the negative impact of the heat capacity of the reservoirs on UCIs?

55 Wetlands of urban areas can have a profound impact on Urban Canopy Layer (UCL) climate levels.
56 Wetlands lower temperature increases, relative humidity, and also lower heat stress index at the downwind side,
57 which is also known as "Lake Effect" (Saaroni *et al.* 2003). "Wetlands include reservoirs, lakes, and rivers, and
58 form many Urban Cooling Islands (UCIs)" (Sun *et al.*, 2012). Most of the UHI studies are implemented at the
59 scale of an entire city. For this reason, there is little information available on the effect of individual wetlands.
60 Various details on the particular wetland, such as the difference of temperature between the wetland and its
61 surrounding landscapes and the transport of cooling effects of wetlands in different spatial scales, are not known.
62 Several works investigated the existence of UCI, the factors having an impact on the UCI intensity and the
63 extent of UCI (Sun *et al.*, 2012, Tominaga et al., 2015, Mitchell et al., 2008, Robitu et al. 2006, Taleghani *et
64 al.*, 2014, Theeuwes *et al.* 2013, Rutherford *et al.* 2004, Rutherford *et al.* 2004, Kim *et al.* 2008, Han *et al.* 2011,
65 Nishimura *et al.* 1998, Manteghi *et al.* 2015, Gupta N. et at 2019, Cheng L., et al. 2019, Xiyan X., et al. 2019,
66 Park C.Y. et al. 2019   and Frey *et al.* 2005). Fraedrich (1972) investigated the existence of the "inversion
67 layer" when the air is blowing from the warmer land over the surface of the waterbody. Inversion increasingly
68 suppresses the evaporation, increasing with the distance traveled over the reservoir by creating a "vapor
69 blanket." Steeneveld *et al.* (2014) suggest that "water bodies might not act as cooling elements in an urban area,
70 especially during the night and evenings in the late summer, due to extensive heat capacity of water bodies
71 compared to their milieu. The shade of Riparian vegetation could counter the negative effect of warming of the
72 stream water and helps ecosystems to adapt (Rutherford *et al.*, 1997).   The positive impact of Riparian shade
73 to moderate air and water temperature also investigated various research work (Johnson *et al.*, 2015, Quinn *et
74 al.* 1997, Rutherford *et al.*, 2004, Bowler et al. 2012, Somers *et al.* 2013, Rutherford et al. 1997, Larson *et al.*
75 1996, Bowler et al. 2012, Sweeney *et al.* 2014). Rosenberg et al. (1983) reported several examples of leading-
76 edge effects at Davis, CA, near Sacramento due to evaporation produced by irrigated fields surrounded by semi-
77 arid areas. Where a step-change in moisture availability had been observed (e.g., Dyer and Crawford, 1965;
78 Goltz and Pruitt,1970; Lang et al. 1974 and Rider et al. 1963). Other significant works on the leading edge or
79 fetch were conducted by Rider et al. 1963, Rijks 1971. Oke (1979) also reported increased evaporation due to
80 microscale advection in urban areas from the study of an irrigated suburban lawn in Vancouver, BC.

81 One of the primary objectives of the creation of "Urban Cooling Island" is to create coolth and transport
82 it inside the urban fabric to achieve a thermally desirable environment in the urban spaces. Through field
83 investigation, Ahmed (1995) established the comfort criteria for the outdoor urban areas of warm-humid cities
84 like Dhaka. One of the requirements for outdoor comfort in the urban spaces of Dhaka were summarized from
85 his work is that "Under still air conditions at an average relative humidity of 70%, for people wearing summer

86   clothing and engaged in sedentary activities or a stationary state, the range of comfort air temperature is between
87   28.5°C to 32°C". The critical parameter which influences the creation of Urban Cooling Island (UCI) is the
88   shading provided to the water of wetland utilizing riparian vegetation and topography of the site. In case urban
89   area, the urban fabric could also be designed in such a way which could act as a shading envelope for the urban
90   wetlands. Also, the Percentage of the built area around the water body, area, shape complexity, and water quality
91   of the water body directly affects the creation of Urban Cooling Island (UCI). Among them, UCI has a two-
92   way relationship with the water quality of the wetland. Based on the literature survey, we prepared the following
93   figure to demonstrate the relation of the different environmental parameters related to the creation of UCI.
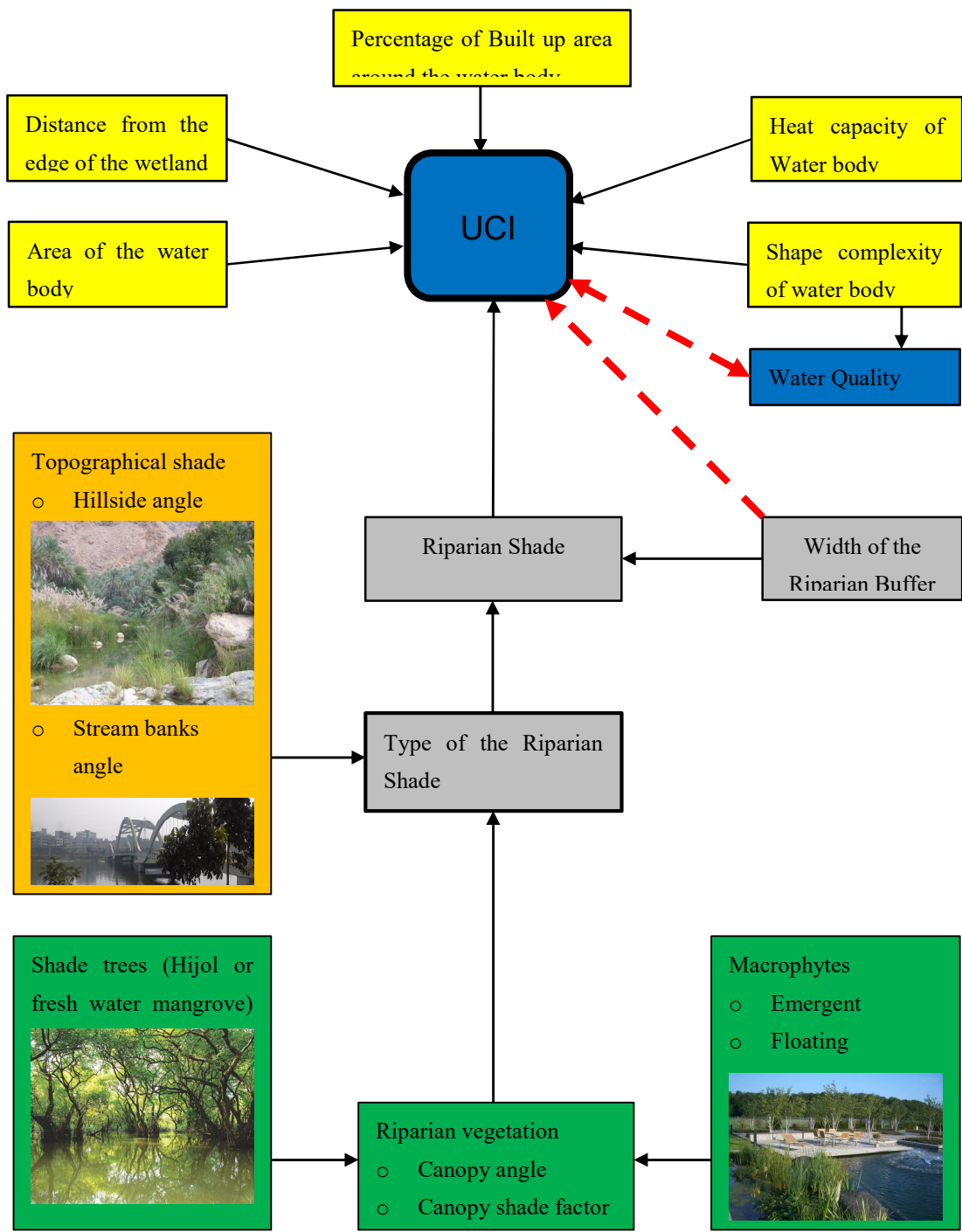94
95
96

97

Figure 1: Relation of the different parameters related to the creation of UCI

98

2. Methodology

Hence, the specific aims of this research were to develop a sustainable path to transform potential wetlands of Dhaka into "Urban Cooling Islands (UCIs)" to address warming issues of Climate Change, which will also promote waterfront ecology with leisure and park amenities as they relate to the urban environment. There is a growing energy crisis in the city due to the high cooling energy demand. Therefore, Urban cooling will be an effective way forward as an adaptation measure against climate change. This multidisciplinary research also aims to form an area of co-existence between natural and humanmade structures in Dhaka.

Objectives of the research

i.   To investigate the factors of Urban Wetland that contribute to Urban Cooling Islands (UCIs) in Dhaka.

ii. To evaluate the impacts of wetland area, shape complexity, location, and riparian shading potential on UCIs intensity in Dhaka.

The research can potentially indicate the parametric relationship between the factors that regulate the Urban Cooling Island (UCI) effect of the wetland at an urban scale. This relationship will give insight to what extent urban wetland design might impact the thermal environment leading to possible Urban Microclimatic cooling. These findings, in turn, might help in the development of a tool for the urban designers and planners to more efficiently manage the Urban Thermal Environment. This research followed the strategy of field study to support simulation and modeling research.

2.1. Field measurement of Urban Cooling Island

The main objective of the field measurement was to determine the morphological characteristics of the Urban Cooling Island (UCI) at the Urban Canopy Layer (UCL). For this reason, the measurement had been carried out in the two study areas at the Urban Canopy Layer (UCL) at the height of 1.5 m to 2 m from the ground. Some measurements were taken on top of the water surface and water edge to determine the effect of water on the air layer above it.

2.1.1. Location of the study area and urban station:

Based on the previous study conducted by the Bangladesh Meteorological Department and Shahjahan et al. (2016), two wetlands of Urban Dhaka were selected for the field study. They were Dhanmondi and Hatirjheel Lake.

The rationale for selecting wetland sites are given below:

a. These two wetlands are accessible up to their inner periphery without any hindrance.

b. Both the wetlands have radiating roads leading into the surrounding urban fabric having the potentials for studying the impact of wetlands on the surrounding area.

c. To enable the analysis of the effect of riparian shade, Dhanmondi Lake was selected for its significantly visible riparian shade, and Hatirjheel lake was chosen for the absence of visible riparian shade.

d. The watershed characteristics of both the lakes are comparable in terms of area.

e. Both the lakes are located on the same physiographic condition (Brammer, 2012) (Details are given in Appendix A). Agro-ecological zone for both the lakes are also the same (FAO/UNDP, 1988).

f. Both the lakes are located in the same overall geothermal gradient zone (Akbar,2011).

The Urban data logging station inside the urban area around these two wetlands were selected with the intent to detect the most significant impact of those wetlands on the microclimate of the encompassing urban fabric. Surrounding areas are uniform or more representative, at least within a half km buffer zone. As per the Urban Climate Zone (UCZ) classification by Oke, 2006, the surrounding urban area of the selected Urban

140   Wetland belongs to UCZ 2. These two existing urban wetlands in Dhaka were studied to discern the
141   relationships among the factors such as UCI intensity and extent, wetland area, shape, location and heat
142   capacity, and Riparian buffer width and type for the Riparian shade of the wetland. A buffer zone of 0.5 km
143   from the edge of the wetlands was taken into consideration for the field measurement. Within the buffer zone,
144   multiple points starting from the water edge to the depth of the urban fabric were selected for microclimatic
145   measurement in line with other studies performed in this field [Sun R. et al., 2012; Robitu M.et al, 2006; Hwang
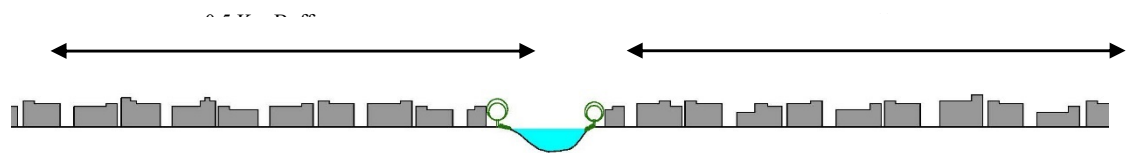146   S.J.et al, 2007].

147

148

149

150

151   Figure 2: Buffer zone for field measurement

152   **2.1.2. Date and time of data logging**

153   Dates for the field measurement were selected from three design seasons of Dhaka, which are Hot Dry
154   (March-May), Warm Humid (June-November), and Cold Dry (December-February). For all the measurements,
155   the sky was mostly free of the cloud with bright sunlight. Data logging was done from morning to sunset on the
156   following dates: at Dhanmondi Lake site on October 21, 2016, and February 24, 2017, at Hatirjheel lakeside on
157   November 11, 2016, and February 10, 2017. One additional data logging was done on December 13, 2016, at
158   the Hatirjheel lake site. On this date, one data logger was simultaneously placed inside Stevenson Screen at the
159   measurement point of Bangladesh Meteorological Department (BMD) at Agargaon together with instruments
160   of BMD from 11 a.m. on December 12, 2016, to 11 a.m. on December 14, 2016, for calibration of the device
161   used in the study, and also as a reference measurement.

162

163   **2.1.3. Observation Period**

164   To investigate 'urban microclimate' dynamics and the "urban heat island," selected observation days were
165   chosen to typify a range of different weather statuses, like the three design seasons in Dhaka, other than rainy
166   days. It was essential to attaining data of high geographical and temporal resolution. But, taking account of our
167   limited budget and human resources, we were only able to collect 12-h samples of data on six occasions, starting
168   from October to February, which was adequate for the research. The variables measured were air temperatures,
169   humidity and wind speed at 1.5–2.0 m height in the middle of Urban Canopy Layer and wetland edge from 7:00
170   a.m. of one day till 6:00 p.m. of the same day, except in one case where the data logger was placed with the
171   Bangladesh Meteorological Department (BMD) instruments for three days for validation purpose. Wind
172   direction and velocity, in our case, were measured just at the edge of the wetland. (Huang, Li, Zhao, & Zhu,
173   2008). Detail information of each urban station of both the site on each measurement day is provided in
174   Appendix A. Description of the instruments used in the measurement is also given in appendix A.

175

176   **2.1.4. Climatic variables measured**

177   Air Temperature (Ta), Relative Humidity (RH), and wind speed (ws) inside and around the selected
178   Urban Wetlands had been measured at selected Urban Stations (Data logging points) by continuous data logging
179   using a Fixed data logger.

180   **2.2. Simulation and modeling**

181   Numerical models quantifying shading by riparian vegetation, topography, and built-form were built.
182 The model was used to estimate the influence of wetlands in the micro-climate of the surrounding area in real
183 situations. The main objective of the simulation work was to determine the morphological characteristics of the
184 Urban Cooling Island (UCI) at the Urban Canopy Layer (UCL). The principal assumption which has been tested
185 in the simulation model is that the water in the wetland will be cooled down with the help of continuous riparian
186 shading to act as UCI; this cooling effect will then be transferred to the urban fabric through the advective
187 process. For this reason, the simulation work was conducted in one of the study areas described in the previous
188 section at the Urban Canopy Layer (UCL), recording the result at the height of 1.5 m to 2 m from the ground.
189 Some measurements were also recorded on top of the water surface and edge of the lake to determine the effect
190 of water on the air layer above it. Data obtained from the field study of the two wetlands were entered into the
191 COMSOL–Multiphysics software as a part of the problem modeling study. Water and Air temperature, Relative
192 humidity, and Wind speed are primary inputs for the simulation besides types of ground cover and the built
193 form. Once the problem modeling is done, the model was projected to test the specific effect of each contributing
194 factor of Urban Cooling Island (UCI) described above. The principal assumption which had been tested in the
195 simulation model was that the water in the wetland would be cooled down with the help of continuous shading
196 and evaporation to act as UCI, which in turn will cool down the air above it and create the high-pressure zone.
197 This cool air will then flow towards the nearest urban center with a low-pressure area owing to the UHI.

198   The modules of the COMSOL-Multiphysics that were combined with modeling the Urban Cooling
199 Island Effect of the urban wetland is:

200   i.   CFD module: Fluid Flow-Single phase flow.
201   ii.   Heat Transfer Module: Heat Transfer in Fluids and Heat Transfer with Surface to Surface Radiation
202   (ht).
203   iii. Chemical Species Transport: Transport of Diluted Species (tds).

204 **2.2.1.   Location and Morphology of the modeling area**

205   An area (approx. 750 m length) adjacent to the Dhanmondi Lake, bounded by road 12A on the North-
206 west, Satmasjid road on the South-west and road 6A on the south-east side was selected for the simulation study
207 as all the data loggers, with one exception, were placed in this zone to collect microclimatic data. Due to the
208 limited computational strength of the computer available for the simulation study, this area was scaled down to
209 a ratio of 1:50. Data obtained from the field measurement of these wetlands were entered into the COMSOL–
210 Multiphysics software as an initial condition of problem modeling study. Water and Air temperature, Relative
211 humidity, and Wind speed are primary inputs for the simulation besides types of ground cover and the built
212 form. Although all the buildings in each block are the detached type, the gaps between the buildings in most of
213 the cases are not more than 2 m. So, for the sake of simplicity of the model, all the buildings in a single block
214 were safely considered as a single building mass. The average building height of the area is approximately 24
215 m. Also, only the part of the lake in the line of prevailing wind direction was modeled. One of the days of field
216 measurement in this area, February 24, 2017, was used for the position of the sun in the simulation model. The
217 simulation time was fixed from 9 a.m. to 4 p.m. on that day. The whole simulation study was conducted for
218 four cases depicting four types of ambient conditions:

219   i.   Case 1: The first simulation study was done with the water of the lake entirely under solar radiation
220   and inlet temperature equal to the maximum temperature of the day obtained from the field
221   measurement.
222   ii.   Case 2: The second simulation study was conducted with the water of the lake entirely under solar
223   radiation and inlet temperature equal to the minimum temperature of the day obtained from the field
224   measurement.

225 iii. Case 3: The third simulation study was conducted with the water body completely shaded from solar
226   radiation and inlet temperature equal to the maximum temperature of the day obtained from the field
227   measurement.
228 iv. Case 4: The fourth simulation study was conducted with the water body completely shaded from solar
229   radiation and inlet temperature equal to the minimum temperature of the day obtained from the field
230   measurement.
231 In all four cases, relative humidity (RH), which is equal to starting RH at 9:00 a.m., was obtained from the
232 field measurement on February 24, 2017.

233 **2.2.2. Computational grid (mesh)**

234 In the COMSOL model, extremely fine mesh settings are used for the simulation model. The five
235 parameters used to set up the mesh in COMSOL are maximum element size 0.9m, minimum element size
236 .009m, maximum element growth rate 1.3, curvature factor .2, resolution of narrow regions 1.5. A
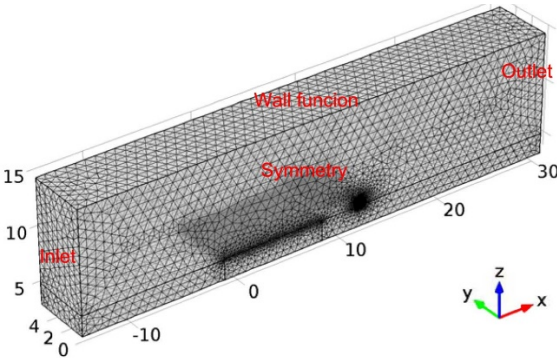237 computational grid of the control domain is given in figure 3.

238

239   Figure 3: Computational grid of control domain

240 From figure 4, a computational grid of the model with its different areas can be seen.
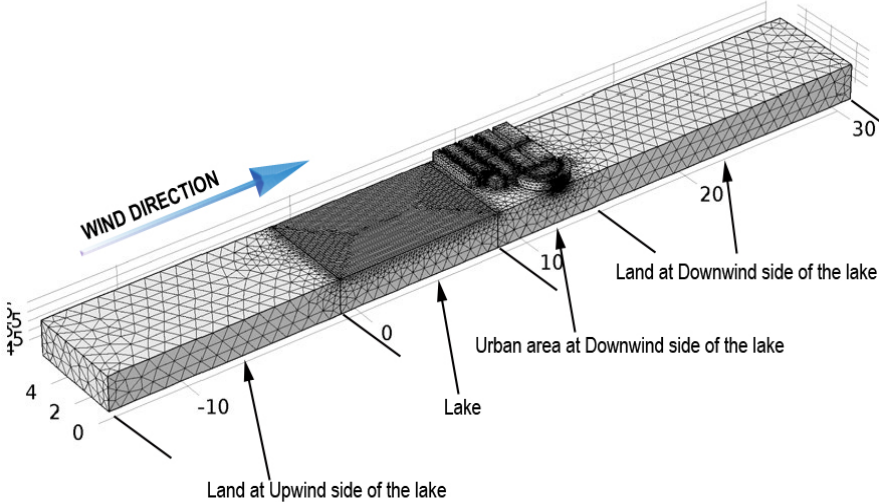

241
242   Figure 4: Computational grid of the model

243 **2.2.3. Boundary Conditions:**

244 Inlet Boundary Condition:

245 Air enters the computational domain at a freestream velocity U_0=.2 m/s normal to the inlet surface.

246 Outlet Boundary Condition:

247 At the outlet, a Pressure condition is applied.

248 Wall Condition:

249 Wall functions describe the floor of the flow domain and surface of the Buildings. Wall functions could also

250 be applied to the outer wall and the ceiling of the Computational domain. Their main effect on the flow

251 around the body is, however, to keep the flow contained, and it will, therefore, suffice to model them as slip

252 walls.

253 Symmetry Condition:

254 Mirror symmetry reduces the computational domain, as shown in Figure 5.

255 Temperature

256 There are three ambient temperature conditions in this model.   First, for case 1, inlet temperature equal to the

257 minimum temperature of the day obtained from the field measurement. Second, for case 2, inlet temperature

258 corresponding to the maximum temperature of the day received from the field measurement. Third, the

259 ground at 1 m below the sand surface is assumed to be at a constant temperature, corresponding to the

260 minimum water temperature at this location for the measurement time of the day, which is from 9 a.m. to 4:00

261 p.m.

262   The modules of the COMSOL-Multiphysics that were combined with Modeling the Urban Cooling

263 Island Effect of the urban wetland were (1) CFD module: Fluid Flow-Single phase flow, Turbulent Flow, k-ω;

264 (2) Heat Transfer Module: Heat Transfer in Fluids and Heat Transfer with Surface to Surface Radiation (ht);

265 and (3) Chemical Species Transport: Transport of Diluted Species (tds). A brief discussion of these modules

266 and roughness parameters are given in appendix B.

267 **2.2.4. Measurement points in the model**

268   Two sets of measurement points had been taken in the model. The first set of seven measurement

269 points at the downwind side of the lake had been chosen to accurately represent the actual urban stations (data

270 logging point) of the field measurement areas around Dhanmondi lake, starting from over the water of the lake,

271 to the edge of the lake, then gradually shifting deeper into the urban fabric. The second set of twenty-two

272 measurement points were taken starting from the land-lake boundary at the upwind side of the lake to the land-

273 lake border of the downwind side of the lake. Most of those points in the second set are at equal distance along

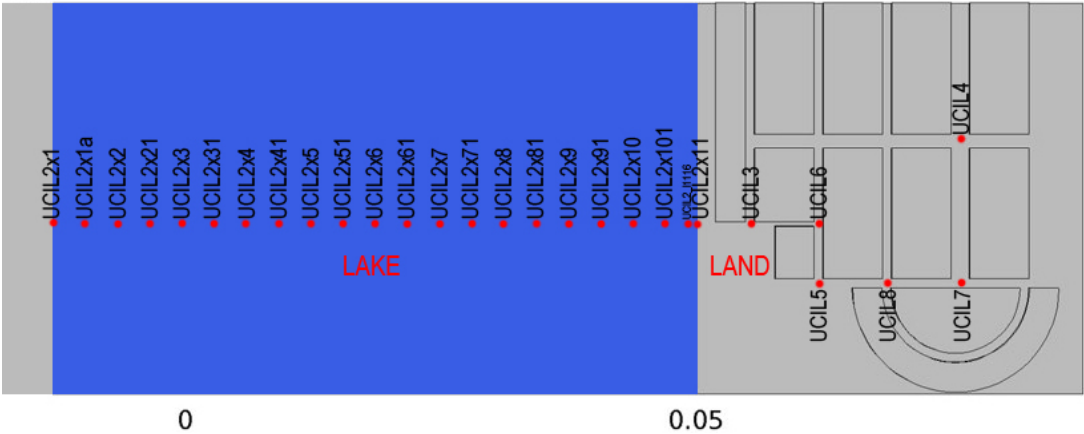274 the length of the lake. All these points are shown in figure 5.

275

276   Figure 5: Measurement points of the model

277 **3.   Results and analysis of Field measurement**

278   The detailed analysis of the result for reference measurement at the Bangladesh Meteorological

279 Department (BMD) is given in appendix C. Both the air temperature and relative humidity in the reference

280 measurement of BMD had shown a strong correlation with cumulative time. Still, the correlation is the opposite

281   for air temperature and relative humidity. When considered as a continuous independent variable rather than a
282   categorical value, time has a cumulative effect throughout the day and night on dependent variables like Air
283   Temperature and Relative Humidity (RH) in terms of solar influx. The strong positive correlational value
284   between cumulative time and air temperature showed that the rate of change in the solar influx is always positive
285   during the daytime. However, the rate of solar influx varies throughout the day. Analysis of the related data
286   from the field measurements at Dhanmondi Lake Hatirjheel Lake urban stations is given in the following
287   sections. Figure 6 indicates in general that the data logger, which is placed further away from the edge of the
288   lake, exhibits more temperature but less humidity in comparison to the data logger located near the lake.
289   However, it is evident from this analysis (figure 6) that this effect is more pronounced in the lake with more
290   Riparian shading (in this case Dhanmondi lake indicated by DM) than the lake with comparatively less shading
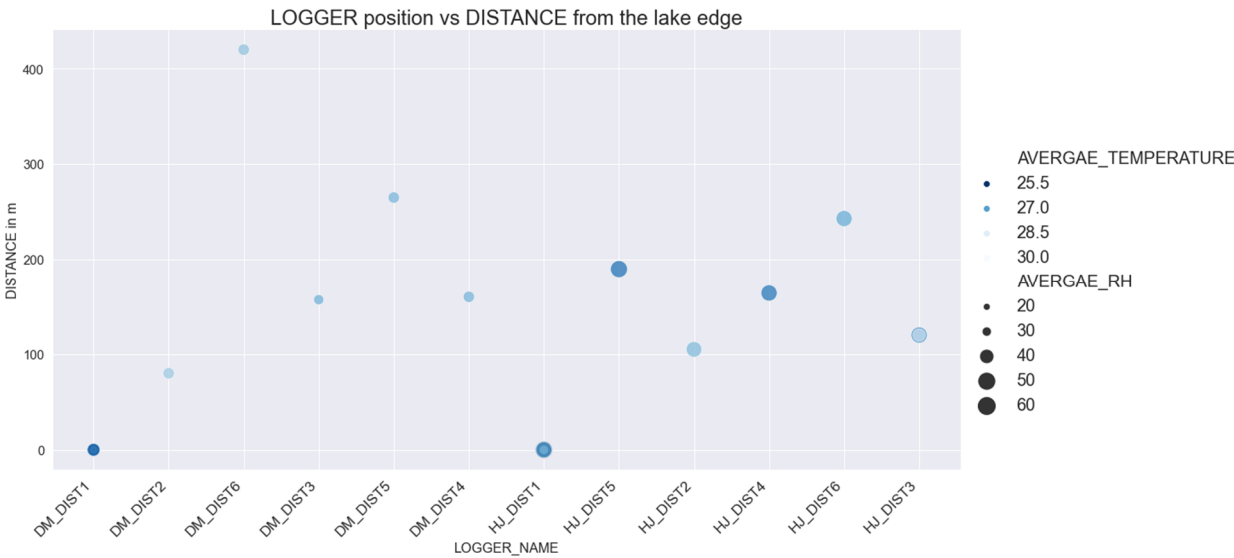291   (in this case Hatirjheel lake shown by HJ)

292

293
294   Figure 6: Relation of Air Temperature and Relative Humidity with the distance from the edge of the lake
295   water

296

3.1 Lake temperature

298   On October 21, 2016, during the greatest hot spell of the day (figure 7), which is at 3:25 p.m., UCILogger4
299   showed a maximum temperature of 35.5°C as it is on a road perpendicular to the wind direction from the lake.
300   Among the urban stations placed on the road parallel to the wind direction, despite being the furthest station in
301   the wind corridor, UCILogger7 was showing the significantly lower temperature of 32.5°C, as it was receiving
302   unhindered wind flow from the lake due to the wide and unobstructed road, whereas wind flow to UCILoggere6
303   (34.0°C) is reduced by trees, small road width, and other small manmade structure. In general, UCILogger4
304   showed higher temperatures throughout the day. The correlation coefficient between air temperature, Relative
305   Humidity, and cumulative time for all the measurement days of the urban stations could be found in Appendix
306   C. Overall; all the urban stations showed a positive correlation between air temperature and cumulative time.
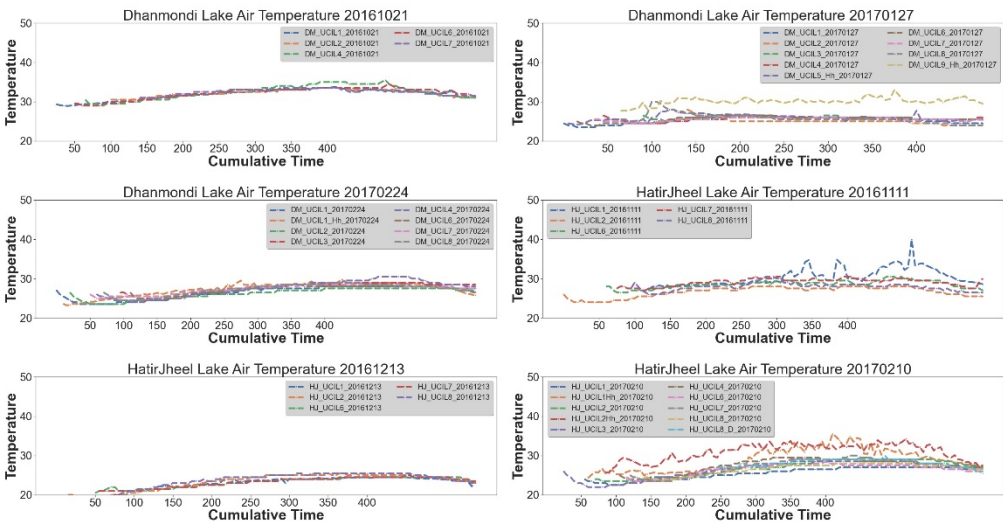
307

308   Figure 7: Air Temperature over the edge and in the surrounding area of the lake at the measurement day

309   Dhanmondi lake Urban stations on October 21, 2016

310   Figure 7 also shows the temperature of the urban stations during the measurement campaign on January

311   27, 2017. Urban stations UCILogger9, located on an island with no riparian shading inside the lake, shows

312   maximum temperature throughout the day. Due to the sky becoming cloudy from 11:00 a.m. onwards on this

313   measurement day, the temperature difference between the different urban stations reduced with respect to the

314   previous measurement day. Even though urban station UCIL9, located in the island middle of the lake, had

315   shown a higher temperature than the other stations throughout the day.   One important thing to observe is that

316   the correlation between air temperature and cumulative time has been significantly changed due to the cloudy

317   sky.   Some urban stations UCIL2, 3, 5, and 8 showed a negative correlation, which indicates the state of heat

318   loss due to the absence of sun. On February 24, 2017. On this day, during the greatest hot spell of the day, which

319   was between 3:35 p.m. to 4:20 p.m., UCILogger4 showed the maximum temperature of 30.5° C as it is in a

320   road perpendicular to the wind direction from the lake. Urban station UCILogger2 showed lower temperatures

321   throughout the day. Among the urban stations placed in the road parallel to the wind direction, UCILogger7

322   and 8 exhibited the higher temperatures of 28.5°C as they were located further away from the lake edge. The

323   maximum temperature of the urban station at the island UCILogger1 is 29°C, which is 0.5°C higher than

324   UCILogger7. In general, UCILogger4 showed greater temperature throughout the day. The correlation analysis

325   between air temperature and cumulative time throughout the day shows heat gain with time for all the urban

326   stations. It is important to note that the urban station at the small island and the water edge was on the higher

327   side in terms of heat gain.

328   The observation result (figure 7) on November 11, 2016, at the Hatirjheel lake Urban stations,

329   demonstrated one of the advective effect named "Oasis effect" in an urban area due to the presence of an urban

330   park. The trees in the park reduced solar gain through shading and evapotranspiration. Otherwise, the Hatirjheel

331   lake area is mostly devoid of significantly large trees for evapotranspiration and shading at UCL. The Urban

332   station UCIL2, located at the edge of the park on the downwind side, showed an overall lower temperature than

333   the others. The urban station UCIL1 showed a higher temperature with some unusual high peak due to the

334   location being on the top of the water of the lake on a bridge without any shading. Also, the passing vehicles

335   were contributing to a sudden peak in temperature. But overall, UCIL1 shows higher temperatures. Despite

336   being inside the fabric and without significant tree shading, UCIL8 showed comparatively lower temperatures

337   due to the canyon shading at the UCL. The correlation analysis between cumulative time and air temperature
338   for all the urban stations on November 11, 2016, showed a moderately positive correlation except for the urban
339   station UCIL8. Being the furthest from the water edge, it proved almost zero correlation, which indicates neither
340   heat gain nor heat loss. One reason is that due to its location on an Urban canopy of the north-south elongated
341   road at this time of the year, it stays mostly in the shade throughout the day. The urban stations in the middle
342   of the lake and water edge showed a moderate correlation, which indicates solar gain throughout the day.
343   On December 13, 2016 (figure 15), one of the urban stations, UCIL8, was at the Bangladesh
344   meteorological department site with their instrument. This was done to consider it as a reference point and for
345   calibration purposes. Among the four Urban stations at the Hatirjheel lake area, three stations UCIL1, 6 & 7,
346   were hung from a bridge in the middle of the lake at a different level from the top of the water surface. UCIL2
347   was placed at the edge of the park-like before, on the downwind side of the park. At the urban stations at the
348   Hatirjheel lake area, UCIL2 showed maximum temperature during the hottest spell of the day. The urban
349   stations in the middle of the water behaved similarly. The correlation analysis from the data of December 13,
350   2016, showed a strong relationship between cumulative time and air temperature in the case of the two urban
351   stations nearest to the top of the surface of the lake water, which indicates positive solar gain. The urban stations
352   at the park also showed a positive solar gain, although this was lesser than the former two. The air temperature
353   data from the observation of the urban stations at Hatirjheel lake on February 10, 2017, are presented in figure
354   16. The minimum temperature at the time of hot spell was 27.5°C at the urban station UCIL6, and the maximum
355   was 30°C at the urban station UCIL7. Urban station UCIL1 in the middle of the lake, hanging on the top of the
356   water, showed a consistent increase in air temperature. However, the temperature stayed below the urban station
357   on the land inside the urban fabric until the afternoon. But it did not decrease like the other urban station on the
358   ground inside the urban fabric in the late afternoon. Urban station UCIL2 at the water edge also followed the
359   pattern of UCIL1. The correlational analysis of the air temperature data and cumulative Time of Hatirjheel Lake
360   urban stations on February 10, 2017, proved that the urban stations on the top of the water UCIL1 and at the
361   edge of the water UCIL2 show the strongest positive correlation of air temperature with cumulative time, which
362   means strong heat gain throughout the day due to the solar influx. This could be explained by the heat capacity
363   of the water, which is higher than the land and air temperature near the water surface regulated by the
364   temperature of the water surface. Water can contain high amounts of heat, and it has a very low albedo. So,
365   with the beginning of the day, it absorbs heat without increasing the temperature quickly, like the urban hard
366   surface. But in the late afternoon, when the urban hard surface starts losing heat and thus decreases its
367   temperature, the water surface does not exhibit similar rapidity in a temperature decrease. It stays relatively
368   warmer than the land till late in the evening, as does the air layer near the water surface. That is why air
369   temperature at the urban stations 1 and 2 are strongly positively correlated with cumulative time, which
370   indicates strong solar gain. The two urban stations at the middle and edge of the urban park, UCIL8 & 3, also
371   exhibited a strong positive correlation between air temperature and cumulative time and thus indicated
372   strong heat gain due to the solar influx. The other three urban stations inside the urban fabric UCIL4, 6 and 7
373   exhibited moderate positive correlation and thus indicated moderate heat gain due to the solar influx. Among
374   these urban stations, heat gain increased with their distance from the water edge.

3.2 Lake relative humidity

376   On this measurement day of October 21, 2016 (figure 11), the minimum humidity was observed throughout the
377   day at the Urban station UCILogger1 at the island inside the lake, which was contrary to the current assumption
378   that humidity near and over the lake should be maximum. The maximum humidity observed throughout the day
379   was at the urban stations UCILogger6 and 7. The urban station at UCILogger4 showed relatively less humidity

380   than UCILogger6 and 7. The correlation calculated from the observation on October 21, 2016, between
381   cumulative time and observed relative humidity (RH) indicates a negative correlation that is consistent with the
382   reference observation made at the BMD site. This negative correlation indicates the positive rate of change in
383   the solar influx throughout the day, which is opposite to the air temperature. For a particular point in the UCL,
384   the more the heat gains due to the solar radiation, the lesser will be the RH. But this positive solar gain could
385   be affected by other factors such as advection and shading from trees or built fabric, which is evident from the
386   observation. From the correlation coefficient, it is evident that the highest solar gain is at the Urban station
387   UCIL1, 4 & 6. The least solar heat gain is on the urban station UCIL7.   As the sky becomes overcast from
388   11:00 a.m. onwards, the Relative Humidity (RH) measurement shows little difference.   The correlation
389   coefficient between cumulative Time and RH calculated from the observation made on January 27, 2017, is
390   presented in table 5, which indicates the heat loss due to the absence of solar influx as the sky became overcast.
391   Usually, in the daytime, the RH is negatively correlated with the cumulative time due to solar influx, although
392   variable. But as the sun disappears behind the cloud, direct solar gain stops immediately, and net radiative loss
393   increases immediately, which is the case in all the urban stations except UCIL4 and 6. UCIL4 and 6 were deep
394   in the urban fabric and devoid of airflow from the lake. But due to heat storage by the fabric, they were still
395   gaining heat although at a much slower rate than before.
396   The observations at the urban stations made on February 24, 2017, are presented in figure 13. In all the urban
397   stations, relative humidity stays in its highest value at the starting of the day, which decreased as the day
398   progressed. The rate of decrease ceased in the late afternoon at approximately around 03:00 p.m. After 04:00
399   p.m., it started to increase till sunset slowly. The lowest humidity observed is 30.5 % at 3:50 p.m. at urban
400   station four, which is the furthest inside the urban fabric.   From the correlation coefficient calculated from
401   February 24, 2017   observation of the urban stations, all the urban stations are showing a negative correlation
402   with humidity change with cumulative time. This indicates heat gain due to solar influx throughout the day and
403   thus the drop in RH. Maximum heat gain and thus increased rate of RH drop was identified at the Urban stations
404   UCIL4 deep in the urban fabric. The second-highest rate of RH drop was observed at the island urban station
405   UCIL1. The UCIL 6, 7, and 8 stations show comparatively less RH drop as they were getting moist air directly
406   from the lake, and the RH drop increased with the distance. From the Relative Humidity (RH) data (figure 8)
407   of the measurement at Urban stations at Hatirjheel lake on November 11, 2016, the overall lowest RH was
408   observed at urban station UCIL1 throughout the day. Overall higher RH was found by the UCIL2 located at the
409   edge of the urban park on the downwind side. Urban station UCIL6 at the water edge also showed overall lower
410   RH throughout the day. The correlation analysis (table 10) between RH and the cumulative time of the data
411   from the urban stations at Hatirjheel lake on November 11, 2016, showed the urban stations at the water edge,
412   top of the water, and the park was negatively correlated with the correlation strength being moderate. The other
413   two stations in the urban fabric also show a negative correlation. UCIL8 showed the least negative correlation
414   for RH, which indicates the least heat gain throughout the day.
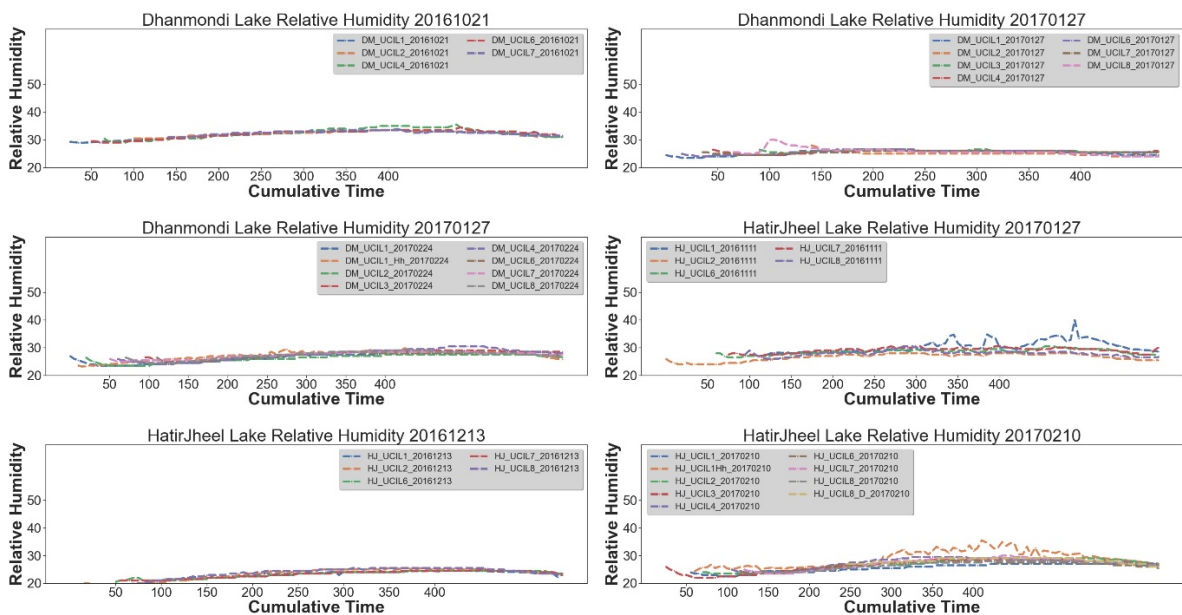415

416

417   Figure 8: Relative Humidity at Hatirjheel lake Urban stations on November 11, 2016

418   Figure 8 shows the Relative humidity data from the urban stations at Hatirjheel lake on December 13,

419   2016. Overall, the first Urban stations on the top of the water surface showed low relative humidity throughout

420   the day.

421   The correlational analysis in between cumulative Time and Relative humidity data from the urban stations at

422   Hatirjheel lake on December 13, 2016, showed a negative correlation throughout the day for all the stations,

423   which is in correspondence with the reference urban station at the BMD site. The negative correlation is strong

424   at the urban stations nearer to water surface UCIL6 and 7. The urban station at the edge of park UCIL2 also

425   shows a strong negative correlation, which indicates strong positive heat gain by air due to solar influx

426   throughout the day. Figure 8 also shows the relative humidity data from the urban stations at Hatirjheel lake on

427   February 10, 2017. Overall, all the urban stations showed a decline of relative humidity as the day progressed,

428   which evened out from the afternoon to late afternoon. Relative humidity again continued to increase slowly in

429   the late afternoon. Urban station UCIL2 at the edge of the water surface started showing lower relative humidity

430   than the other stations starting from the afternoon till sunset. The humidity at the urban station UCIL1 on top

431   of the water surface declined relative to other urban stations on the ground from the afternoon till sunset. The

432   correlational analysis   between cumulative time and relative humidity data of the urban stations of Hatirjheel

433   lake on February 10, 2017, is presented in Table 15 indicates an overall negative correlation at all urban stations.

434   This correlational analysis clearly showed the strongest negative correlation between cumulative time and

435   relative humidity at the urban station on top of the water UCIL1 and at the water edge UCIL2, which indicates

436   a decrease in relative humidity due to the high heat gain of water due to solar influx throughout the day. The

437   urban stations in the middle of park UCIL8 and at the edge of the park UCIL3 also showed a strong negative

438   correlation. The other three urban stations inside the urban fabric UCIL4, 6 &7, also showed a strong negative

439   correlation, although to some lesser extent than the previous four stations at the top of the water and the park

440   near the water edge.

441

442   **3.3 Key observations from Field Measurement**

443   Several important observations could be made from the analyzed field measurement data obtained

444   from the selected urban stations on both the wetlands discussed in the previous section.

445 **i.   Effect of cumulative Time on the rate of change of air temperature and relative humidity**

446 The study shows that time, if considered as an increasing quantity rather than a categorical value, has
447 a cumulative effect on the rate of change of air temperature and relative humidity in terms of solar influx. At
448 night, due to the absence of solar influx, the air temperature has an almost negative linear relationship with
449 cumulative time and relative humidity (RH) has a nearly positive linear relationship with cumulative time.
450 During the day, with the presence of solar influx, although variable, the time cumulative effect is reversed. In
451 the daytime, the air temperature has a strong positive correlation with cumulative time, and Relative Humidity
452 has a strong negative correlation with cumulative time.

453 **ii.   Effect of riparian shading on the cumulative time effect**

454 In the case of urban wetland devoid of riparian shading, the cumulative effect of time is strongest at
455 the top and near the edge of the wetland, which is evident from the analysis of the field data measured at
456 Hatirjheel lake urban stations. In the case of the Dhanmondi lake area, the cumulative effect of time is relatively
457 weaker than that of the Hatirjheel lake area.

458 **iii.   Influence of the distance from the edge of the wetland on temperature**

459 Air temperature drops in those urban stations which are located on the road parallel to the wind flow
460 from the wetland when the built forms or natural features do not obstruct the wind flow. This effect is more
461 pronounced in the case of Dhanmondi lake than Hatirjheel lake. The temperature on the urban station increases
462 with distance from the lake edge. The urban station located on the road perpendicular to the prevailing wind
463 direction from the lake exhibits a higher temperature.

464 **iv.   Effect of the location of the park on temperature**

465 The existence of an urban park creates an "oasis effect" by moderating temperature and increasing
466 humidity, which is the case in the Hatirjheel Lake area. Hatirjheel lake is mostly devoid of large vegetation in
467 its surroundings. But the existence of the urban park creates a small "oasis effect."

468 **v.   Effect of shading in the urban canyon**

469 Urban stations which are located in the urban canyon shaded most of the time by the canyon itself
470 showed decreased temperature.

471 **vi.   Humidity and distance from the lake edge**

472 Relative humidity (RH) near the edge of the water and over the water is lower than the park and
473 vegetated area, which is consistent with the findings of Geiger (2009).

474 **vii.   Evaporative cooling potential**

475 Another important observation is that with the progress of the day, relative humidity decreases, which
476 dips significantly from mid-day to late afternoon. This phenomenon of the relative humidity increases the
477 evaporative cooling potential.

478 **4.   Results and Analysis of Simulation Study**

479 The detailed analysis of the data from the simulation results is given in the following sections.

480 **4.1 Effect of Shading on Water Temperature**

481 A simulation study had been conducted at a section of the Dhanmondi Lake area (approx. 468 m × 280
482 m) adjacent to Satmasjid road (on South-west), and road 6A (on the south-east) has been selected. One of the
483 days of field measurement in this area, February 24, 2017, was used for the sun position in the simulation model.
484 The simulation time was fixed from 9 a.m. to 4:00 p.m. of that day. The whole simulation study was conducted
485 for three cases depicting three types of ambient condition:

486 a.   Case 1: First simulation study conducted with the water of the lake entirely under solar radiation.

487   b.   Case 2: Second simulation study conducted with the fifty percent (50%) water of the lake under solar

488   radiation.

489   c.   Case 3: Third simulation study conducted with the water body completely shaded from solar radiation.

490   The simulation was conducted using COMSOL-Multiphysics software version 5. Heat Transfer

491   Module - Heat Transfer with Surface to Surface Radiation (ht) of COMSOL -Multiphysics was used in the

492   simulation. The initial temperature of the water was fixed at the level equal to the minimum temperature of the

493   day obtained from the field measurement. Detail description of the model is given in section 2.2. Below, figure

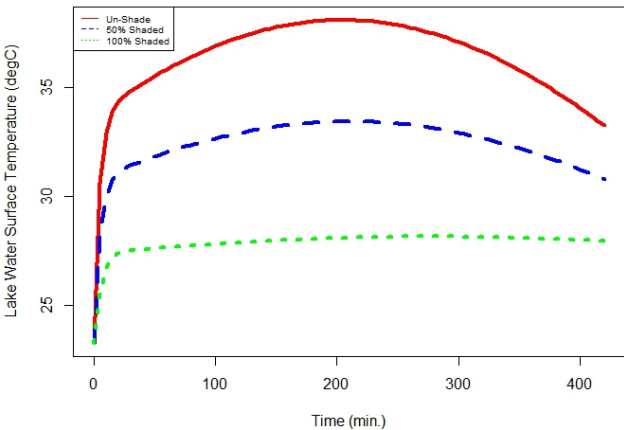494   9 depicts the effect of shading on the water surface temperature of the lake.

495

496   Figure 9: Effect of shading on simulated water surface temperature of the lake

497   From the simulation study, it could concur that the fully shaded water surface reacted little to the

498   progressing day temperature as, in this case, the waterbody can only gain heat from the ambient temperature of

499   the atmosphere.

4.2 Effect of cumulative Time on the rate of change of air temperature and relative humidity

501   When time is considered as a continuous variable rather than a categorical value, we get the cumulative

502   effect of time on the rate of change of air temperature and relative humidity. Temperature and Relative humidity

503   (RH) data at the first set of seven points in each of the four cases were extracted, and correlation analysis was

504   done in the R-studio using R programming language considering time as a continuous independent variable to

505   see its cumulative effect. In the first case water, of the whole lake was under complete solar radiation with inlet

506   temperature equaling the maximum temperature of the day. In the second case, the water of the entire lake was

507   under full solar radiation, with inlet temperature equaling the minimum temperature of the day. In the third case,

508   the water of the whole lake was shaded entirely from solar radiation with inlet temperature equaling the

509   maximum temperature of the day.   In the fourth case, the water of the entire lake was wholly sheltered from

510   solar radiation with inlet temperature equaling the minimum temperature of the day.

511
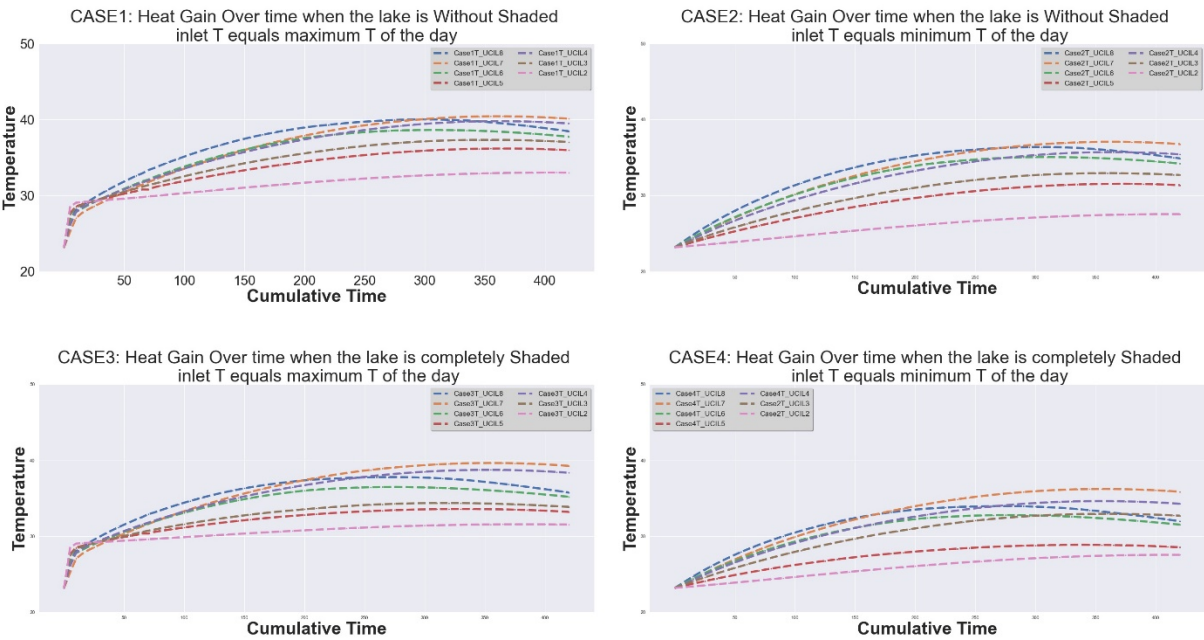
512

513   Figure 10: Effect of shading on simulated water surface temperature of the lake

514   The correlation analysis of the four cases strongly corresponds with the result of field measurement at

515   the two lake-areas and reference measurement at the Bangladesh Meteorological Department (BMD). It has

516   been observed from the field study that the time is considered as a continuous variable (an increasing quantity

517   rather than a categorical value), has a cumulative effect on the rate of change of air temperature and relative

518   humidity in terms of solar influx. In all four cases, the rate of change in air temperature strongly and positively

519   correlated with time (figure 10). In the case of Relative Humidity, it is mostly negatively correlated, with the

520   measurement point deep inside the urban fabric (UCIL4 and UCIL7) showing the strongest negative correlation.

521   The measurement points near and over the water of the lake revealed a weak negative or weak positive

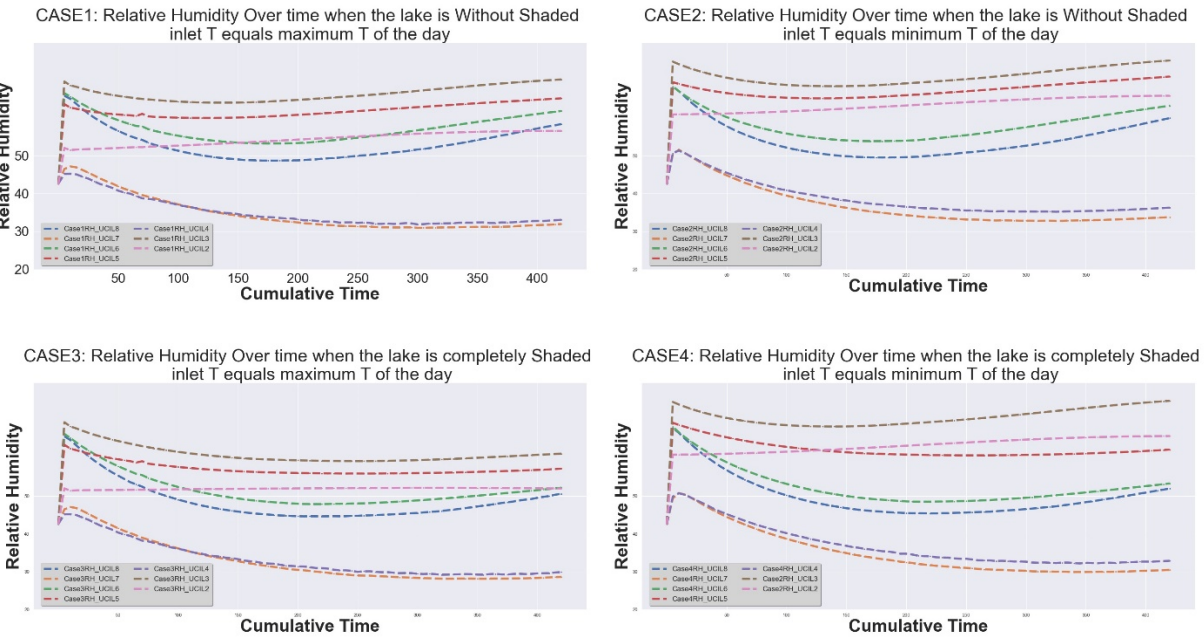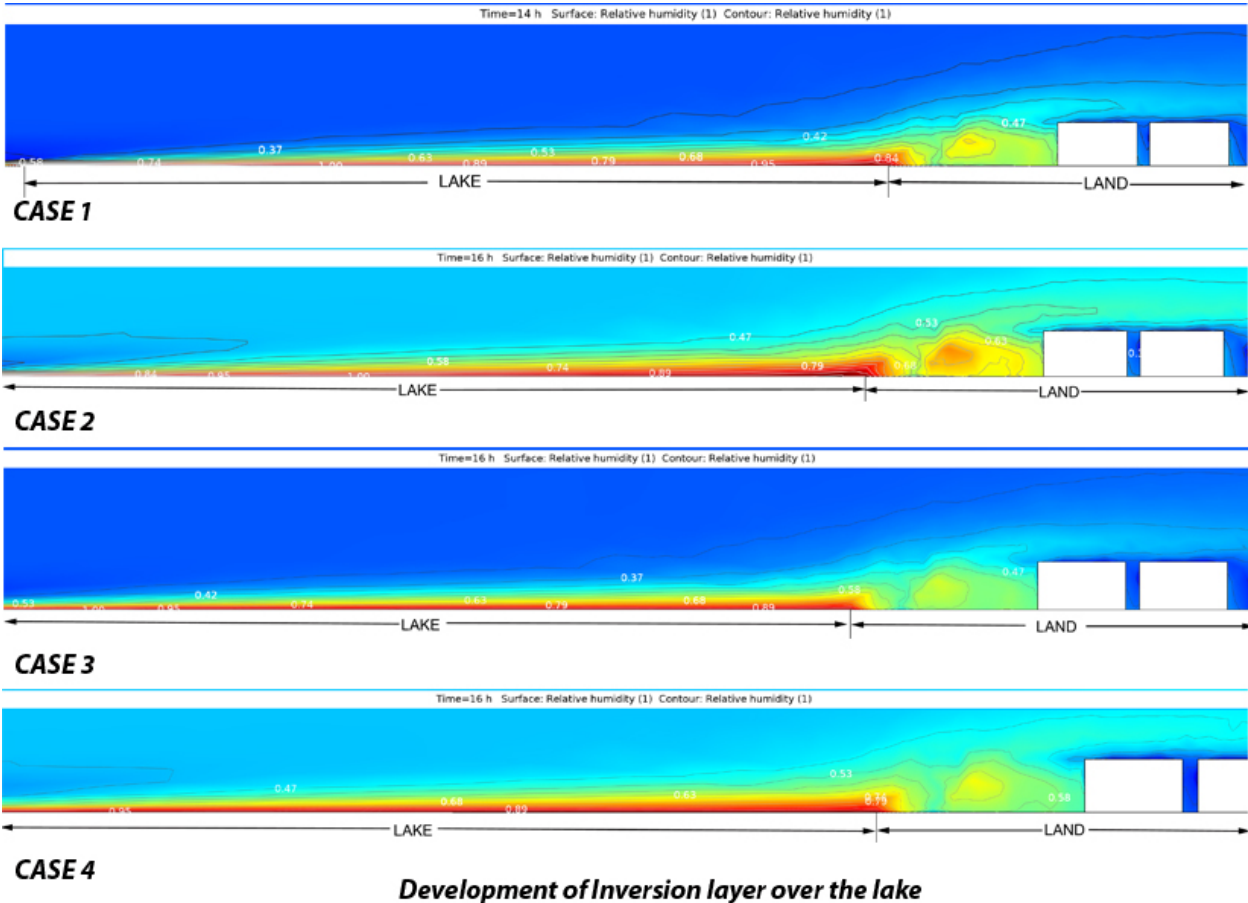522   correlation with time, which corresponds to the field measurement of both the lake- areas. (figure 11).

523

524
525

526   Figure 11: Effect of shading on simulated Relative Humidity above the water surface of the lake

527

528   **4.3 Development of inversion layer**

529   Fraedrich (1972) observed a shallow, stably stratified layer over the water of the lake, which he named
530   the "inversion layer." This layer is produced by a negative downward flux over a water surface when the air is
531   blowing from the warmer land. Also, if the advected air is relatively dry, evaporative cooling amplifies the
532   stable inversion layer. The inversion can also happen even if the air temperature of the environment is equal or
533   less compared with the temperature of the water surface at the shore. The reason for this is that the interaction
534   between the air and the water varies (decreases) the water surface temperature along the air trajectory. The
535   inversion layer also increasingly suppresses the evaporation from the lake, which increases with the travel
536   distance of the air over the lake by creating a "Vapor blanket."
537   All these phenomena mentioned above observed by Fraedrich were demonstrated in the four cases of the
538   simulation study. All the conditions of the creation of the "inversion layer" have been covered by the four cases
539   of the simulation study.
540   **Case 1:** In the first case, the water of the whole lake was under complete solar radiation with inlet temperature
541   equaling the maximum temperature of the day. The starting Relative Humidity (RH) of the simulation was set
542   at equal of the RH observed at 9:00 a.m. on February 24 in the Dhanmondi lake area. The simulation showed
543   (figure 12) a clear inversion layer above the water surface of the lake. The inversion layer is slightly advected
544   towards the downwind side of the lake above the ground.

545
546   Figure 12:   Inversion layer above the lake
547

548   **Case 2:** In the second case, the water of the whole lake was under complete solar radiation with inlet temperature
549   equaling the minimum temperature of the day. The starting Relative Humidity (RH) of the simulation was set
550   equal to the RH observed at 9:00 a.m. on February 24 in the Dhanmondi lake area. The simulation showed

551 (figure 12) a clear inversion layer above the water surface of the lake. The inversion layer is slightly advected
552 towards the downwind side of the lake above the ground.

553 **Case 3:** In the third case, the water of the whole lake was shaded entirely from solar radiation with inlet
554 temperature equaling the maximum temperature of the day. The starting Relative Humidity (RH) of the
555 simulation set equal to the RH observed at 9:00 a.m. on February 24 in the Dhanmondi lake area. The simulation
556 showed (figure 12) a clear inversion layer above the water surface of the lake. The inversion layer is slightly
557 advected towards the downwind side of the lake above the ground, although this advection is less than case 1
558 and 2. Also, the thickness of the inversion layer is less than case 1 and 2.

559 **Case 4:** In the fourth case, the water of the whole lake was shaded entirely from solar radiation with inlet
560 temperature equaling the minimum temperature of the day. The starting Relative Humidity (RH) of the
561 simulation set equal to the RH observed at 9:00 a.m. on February 24 in the Dhanmondi lake area. The simulation
562 showed (figure 12) a clear inversion layer above the water surface of the lake. The inversion layer is slightly
563 advected towards the downwind side of the lake above the ground, although this advection is less than case 1
564 and 2. Also, the thickness of the inversion layer is less than case 1, 2 & 3.

565 **4.4 Effect of the fetch on the inversion height**

566   A strong relationship between the inversion height and the fetch had been observed in all the four
567 cases. Fetch is the distance starting from the land-lake boundary of the downwind side of the lake to the upwind
568 side towards the wind flow direction. Inversion height is the maximum thickness of the inversion layer (fully
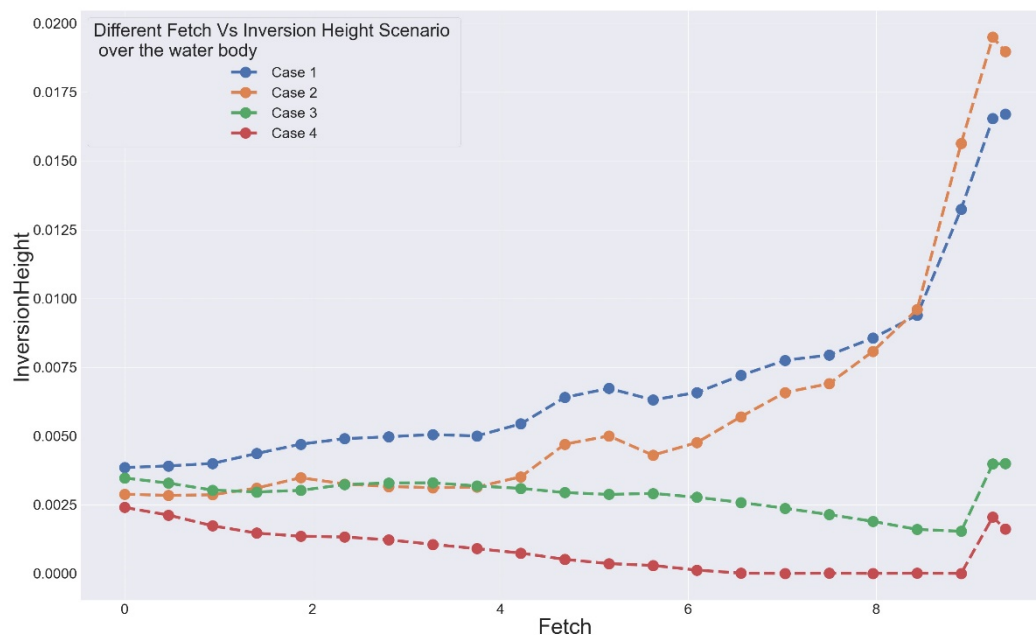569 saturated with water vapor) at a particular point over the lake (Figure **13).**

570
571   Figure 13: Case 1 - Inversion height z versus fetch x
572

573 **Case 1:** In the first case, the water of the whole lake was under complete solar radiation with inlet temperature
574 equaling the maximum temperature of the day. In this case, the inversion layer increases in height with the
575 increasing fetch (figure 13).

576 **Case 2:** In the second case, the water of the whole lake was under complete solar radiation with inlet temperature
577 equaling the minimum temperature of the day. In this case, the inversion layer increases in height with the
578 increasing fetch (figure 13), although this increase is less than case 1.

579   **Case 3:** In the third case, the water of the whole lake was shaded entirely from solar radiation with inlet
580   temperature equaling the maximum temperature of the day. In this case, the inversion layer decreases in height
581   with the increasing fetch (figure 13).

582   **Case 4:** In the fourth case, the water of the whole lake was shaded entirely from solar radiation with inlet
583   temperature equaling the minimum temperature of the day. In this case, the inversion layer decreases in height
584   with the increasing fetch (figure 13).

585   **4.5 Correlation between the Inversion height and fetch:**

586   Table 20 in Appendix C shows the correlation between the inversion height and fetch. In the case of
587   Cases 1 and 2, inversion height has a strong positive correlation with fetch, with Case 1 having the strongest
588   positive correlation. Whereas in the case of Cases 3 and 4, the correlation is negative, with Case 4 having the
589   strongest negative correlation.

590   This correlational analysis demonstrates the effect of riparian shading on the water temperature of the
591   lake and hence the thickness of the inversion layer. It is clear from the study that Urban wetlands with shade
592   and less warm wind flow from the upwind will have a thinner inversion layer than the wetland with no shading
593   and warmer inflow. Also, relative humidity (RH) above the inversion layer of the lake will be less even
594   compared with that of the land. This is the reason why in the field study, the urban stations over the water of
595   the lake and the edge of the lake showed lower Relative Humidity (RH) compared to the urban stations deep
596   inside the fabric. Because, on average, urban stations above the water surface and edge of the lake were placed
597   approximately 6 m above the water, those urban stations were above the inversion layer and hence showed
598   lower RH.

599   **4.6 Inversion model**

600   A linear regression model has been built based on the simulation model to test the relation between
601   fetch, inversion layer thickness, temperature, and the horizontal component of total energy flux in the inversion
602   layer. All the four cases described in this section are considered in the regression analysis. The variables
603   included are:

604   i.   Independent variable: Fetch (x)
605   ii. Dependent variables: Inversion height (z), Air temperature (T), Relative humidity (RH), the
606   horizontal component of the total energy flux (f).

607   From the simulation data, all the values of the variables are selected for fully saturated air, i.e., 100%
608   relative humidity. The regression analysis is done on the R-studio using the "R" programming language. The
609   following are the regression models that describe the relationship:

610   **Case 1:** For Case 1, the regression model is:

611    $$x = 39.42 + 868.6928z - 1.319T + .003547f$$

612   From the model, it is evident that if the T and f are unchanged, increasing fetch will increase the
613   inversion layer thickness.

614   **Case 2:** For Case 2, the regression model is:

615    $$x = 43.02 + 740.7z - 1.321T + .00004596f$$

616   From the model, it is evident that if the T and f are unchanged, increasing fetch will increase the
617   inversion layer thickness, although the increase will be less than that of Case 1.

618   From these two models, it is clear that we have to reduce fetch to reduce the thickness of the inversion
619   layer and thus promote heat exchange between water and the air blowing above it. To reduce fetch, longer
620   direction or length of the wetland should be perpendicular to the prevailing wind direction.

621   **Case 3:** For Case 3, the regression model is:

622
$$x = 3.317 - 491.1z - .3212T + .00004596f$$

623   From this model, it is evident that if the T and f are unchanged, increasing fetch will decrease the
624 inversion layer thickness.

625   **Case 4:** For Case 4, the regression model is:

626
$$x = -17.74 - 305.93952z + 1.0244T - .01463f$$

627   From the model, it is evident that if the T and f are unchanged, increasing fetch will decrease the
628 inversion layer thickness. This reduction will be higher than that of Case 3.

629   Form these four models; it is evident that in an unshaded wetland, increasing fetch will increase the
630 depth of the inversion layer. However, in a shaded wetland, increasing fetch will decrease the depth of the
631 inversion layer, as the inversion layer decreases with increasing fetch and thus promotes heat exchange between
632 water and the air blowing above it.

633   **4.7 Effect of the relative humidity on the inversion layer thickness**

634   Two additional scenarios of relative humidity were considered for testing the relationship between the
635 inversion height and the relative humidity both with Case 1 and Case 3 described previously.

636   Case 1: In the first case, the water of the whole lake was under complete solar radiation with inlet
637 temperature equaling the maximum temperature of the day. Relative humidity (RH) was equal to the starting
638 RH obtained from the field measurement at 9:00 a.m., which was 51.5%. In the first scenario of Case 1, the
639 initial RH is set to 1.5 times of RH of the field measurement, which is 77.25%. In the second scenario of Case
640 1, the initial RH is set to 0.5 times of RH of the field measurement, which is 25.75%. The results obtained in
641 the two scenarios of case 1 are plotted below in figure 14. The results indicate the increase of the inversion layer
642 thickness with increasing humidity from the upwind flow.

643   Case 3: In the third case, the water of the whole lake was shaded entirely from solar radiation with
644 inlet temperature equaling the maximum temperature of the day. Relative humidity (RH) was equal to the
645 starting RH obtained from the field measurement at 9:00 a.m., which is 51.5%. In the first scenario of Case 3,
646 the initial RH is set to 1.5 times of RH of the field measurement, which is 77.25%. In the second scenario of
647 Case 3, the initial RH is set to 0.5 times of RH of the field measurement, which is 25.75%. The results obtained
648 from the two scenarios of Case 3 are plotted below in figure 14. The results indicate the increase of the inversion
649 layer thickness with increasing humidity from the upwind flow, although the water surface is entirely under
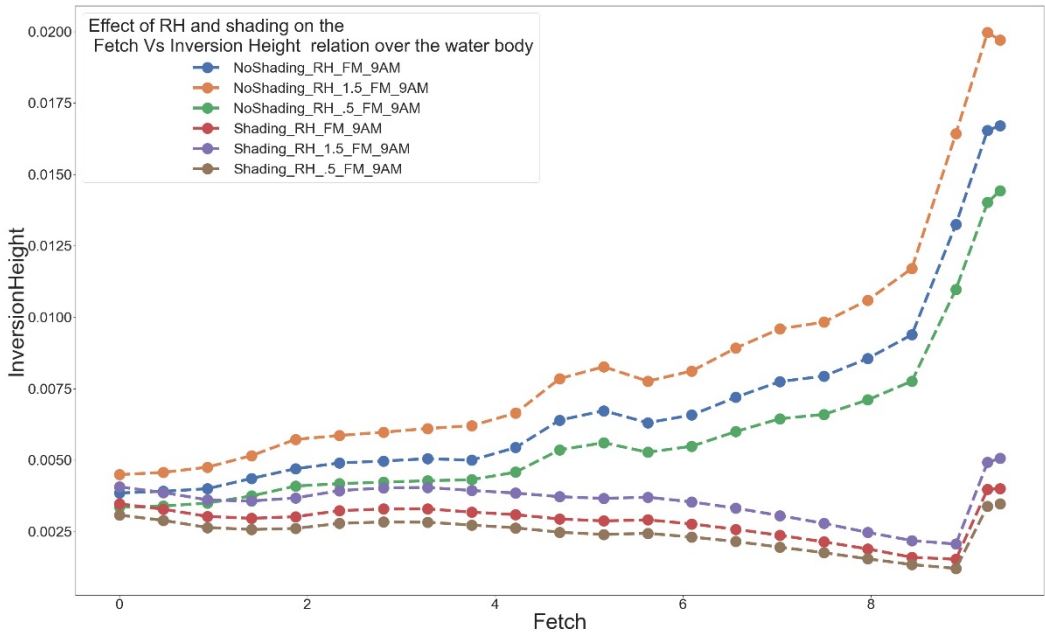650 shading.

Figure 14: Case 1 - Effect of relative humidity (RH) on inversion height

4.8 Effect of the orientation and riparian shading height of the wetland on the water temperature

The effect of orientation and shading height on the water surface temperature was simulated. The simulation time was 9:00 a.m. to 4:00 p.m. (Figure 15).
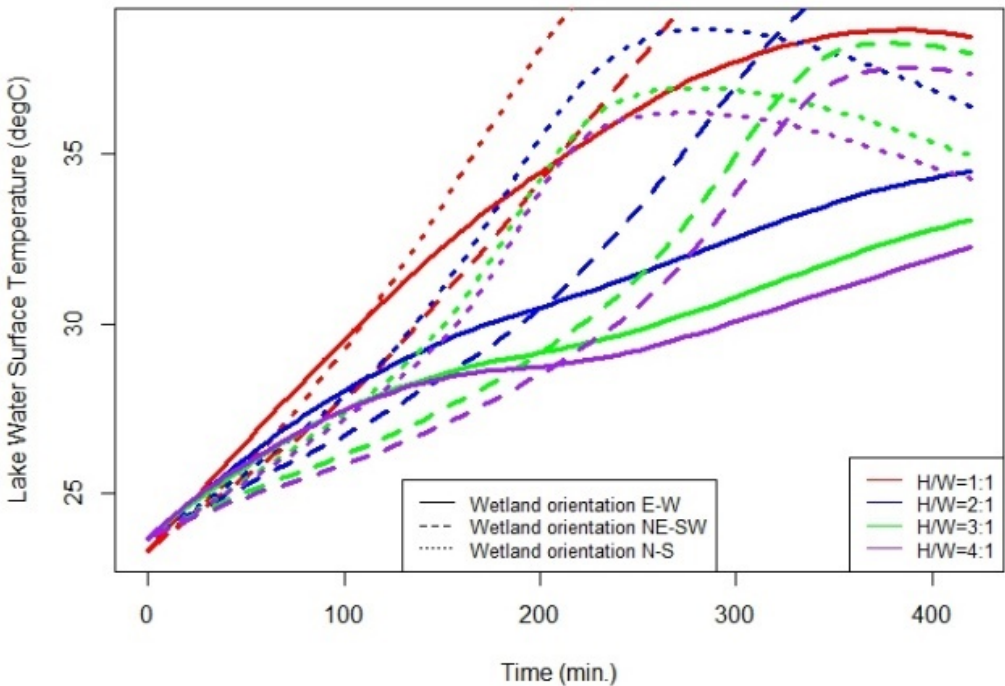

Figure 15: Effect of wetland orientation and the ratio of shading height (H) vs. water surface width (W) on the temperature of the water surface.

The date of the simulation was considered as February 24 to maintain consistency with the field measurement date of the Dhanmondi lake area. For this simulation, a hypothetical wetland of linear shape with shading on both sides was considered. Four ratios between the shading height (H) and wetland water surface width (W) were found in conjunction with three orientations of the wetland. The ratios were H/W=1, H/W=2, H/W=3, and

664 H/W=4.   The three orientations of the long axis of the wetland considered were East-West (90°), North/East-
665 South/West (45°), and North-South (0°). The result of the simulations is given in figure 31. It can be concluded
666 from figure 15 that for the same amount of shading if the long axis of the wetland is oriented towards East-west
667 (i.e., the wetland is more elongated towards East-West than North-South), it will be shielded more from the
668 direct solar radiation, hence heat gain will be less. Wetland with a long North-South axis is less desirable in
669 terms of shading from direct shortwave radiation from the sun. Although the increase in H/W ratio will provide
670 better shielding against the direct solar radiation, together with the correct orientation, this high H/W ratio will
671 create optimal shading for the water of the wetland. Also, beyond H/W ratio 2, a further increase in shading
672 height will not bring significant benefit in terms of controlling the temperature of the water surface.

673 **5. Conclusions**

674 Urban wetlands are of paramount importance for their environmental functions besides their role in improving
675 the aesthetic characteristics of urban places. But to use the wetland in the urban fabric without considering its
676 wide range of physical and morphological characteristics might create an unfavorable urban environment or
677 may result in a loss of opportunity. Shading is essential for the wetlands of urban areas in the tropics. Without
678 necessary shading, the urban wetland will cease to play its role as a source of coolth for the urban fabric. Shading
679 of the urban wetland could be achieved through typography, urban built form, and riparian shading. The
680 research work demonstrated the effect of differential shading pattern on the relation between fetch and inversion
681 layer thickness, opening avenues for designing retrofitting measures for architects, urban designers, and
682 planners by way of landscaping interventions and modifications or amending building codes. So, an urban
683 wetland with adequate riparian shading can render its essential role as "Urban Cooling Island (UCI)." Based on
684 the findings of the research an urban design matrix for urban wetlands was developed (Given in appendix D),
685 which can contribute to design and planning thermally desirable urban bioclimate imperative in the warm-
686 humid conditions of urban Dhaka as an adaptation measure against climate
687 change. The effectiveness of the urban design guidelines presented in the design matrix for urban wetlands can
688 help improve the bioclimate significantly if they form a part of the overall urban design scheme and urban
689 development policy.

690 **6. Suggestions for Further Work**

691   Further works are required to investigate the behavior of urban wetlands in terms of its heat exchange
692 with the atmosphere and with the land. This works needs to be carried out in the following two forms:
693   i.   **Field measurement:**
694 Field measurement is required at multiple points, both at the horizontal and vertical direction, to capture the
695 character of the inversion layer in detail. This measurement needs to be carried out on both diurnal basis and
696 throughout the whole year in different seasons. In this study, the measurement point was only one or two points
697 at the top and edge of the water with no robust measurement to capture the vertical profile of the variables, and
698 this needs to gap in measurement needs to be addressed.
699   ii.   **Simulation work:**
700 Due to the limited computational resources, the simulation model of the urban area was scaled down to a ratio
701 of 1:50 and also simplified. So, to get an accurate understanding of the heat exchange mechanism of the urban
702 wetland with its surroundings and atmosphere, a full-scale model simulation with as much possible detail is
703 required. Also, the evapotranspiration of the tree has not been included in the simulation model, which must be
704 included to get an accurate scenario of the urban environment.

705   **Supplementary Materials:**

706   An appendix is uploaded with this manuscript containing necessary information of the research. All data
707   generated or analyzed during this study are included in this published article (and its Supplementary Information
708   files). The research data could be downloaded from the BUET Institutional Repository at the following web
709   address:

710   http://lib.buet.ac.bd:8080/xmlui/handle/123456789/4901

711   **Author Contributions:** Abu Taib Mohammed Shahjahan wrote the main manuscript text, prepared all figures
712   and tables. All authors reviewed the manuscript.

713   **Funding:** This research received no external funding.

714   **Acknowledgments:** This paper is drawn from the Ph.D. research at the Department of Architecture, Bangladesh
715   University of Engineering and Technology (BUET). Also, this paper was presented in a poster form in the
716   "Symposium on Challenges in Applied Human Biometeorology that will take place on March 2 and 3, 2020 in
717   Freiburg, Germany". The principal author received a travel grant from the Tromp Foundation to present the
718   poster in the above-mentioned Symposium.

719   **Conflicts of Interest:** The authors declare no conflict of interest.

720   **Appendix A**

721   **Characteristics of the urban stations:**

722

723   **Dhanmondi Lake Urban Stations:**

724   The locations of the urban stations chosen for field measurement are shown on the Google Earth
725   image (figure3). In the case of Dhanmondi lake, all the urban stations except one (UCILogger4) were installed
726   along the path of prevailing wind direction from the lake. The urban station UCILogger4 was placed in a road
727   deep inside the urban fabric which was perpendicular to the prevailing wind direction. One urban station,
728   UCIlogger1, was placed on a small island inside the lake.

729

730   Figure 16: Location of the Urban stations of field measurement at Dhanmondi Lake on 24 February 2017

731   Detail information of each urban station on each measurement day of the Dhanmondi Lake area provided in
732   Table 1 of Appendix A in "data in brief".

733

734

735   The following table (Table 1) provides detail information of each urban station on each measurement day of
736   the Dhanmondi Lake area.

737   Table 1: Data Logger Location at Dhanmondi Lake area, 24 **February** 2017

Sl	Logger Name	Location and Physical Characteristics of location	Location Photo	Geographical Co-ordinates	Duration of the Data Logging
1	UCILogger1	Island in between road 6A and Sudha Sadan. Ventilated Box mounted. On the edge of a small island, in the middle of the lake under tree shade. 1 m from the ground surface, tied with a branch of shrubs		Latitude 23.743302 Longitude 90.377449	Start 7:35 a.m. Finish 6:00 p.m.
2	UCILogger1 - Extech Dual Sensor	Island in between road 6A and Sudha Sadan. Handheld. On the edge of a small island, in the middle of the lake under tree shade. 1 m from the ground surface, tied with a branch of shrubs		Latitude 90.377449 Longitude 23.743302	Start 7:45a.m. Finish 6:00 p.m.
3	UCILogger2	Rabindra Sorobor; water edge; tied to the branch of a banyan tree. Ventilated Box mounted. 0.8 m from the top of the water surface.		Latitude 23.744261 Longitude 90.376882	Start 7:55 a.m. Finish 6:00 p.m.
4	UCILogger2 - Extech Thermo-anemometer	Rabindra Sorobor water. Handheld. 1.5 m from the top of the ground surface.		Latitude 23.744261 Longitude 90.376882	Start 11:50 a.m. Finish 6:00 p.m.
5	UCILogger3	Rabindra Sorobar restaurant, Junction of road 7A. Ventilated Box mounted (at 1.8 m height) under the shade of a tree, exposed to direct air from the lake; 80 m from the edge of the water in North-western direction.		Latitude 23.745408 Longitude90.376686	Start 9:10 a.m. Finish 6:00 p.m.
6	UCILogger4	the crossing of Road 8A &10A. Ventilated Box mounted (at 1.8 m height) in a partly grass-covered ground surface under the shade of a tree, Deep in the urban fabric with no direct air corridor from the lake to the point. Approximately at a distance of 420 m directly from the edge of the lake water in the North-Eastern direction (heading 112 degrees).		Latitude 23.747157 Longitude 90.373729	Start 8:32 a.m. Finish 6:00 p.m.

7	UCILogger6	Road 8A near Rabindra Sorobor. Ventilated Box mounted (at 1.8 m height) on paved footpath under the shade of a tree; two air corridors from the lake: 120 m from the edge of the water in North-Eastern direction. 120m in South-Eastern direction.157m directly from the edge.		Latitude 23.745942 Longitude 90.376096	Start 9:25 a.m. Finish 6:00 p.m.
8	UCILogger7	Junction Road 10A & Sultana Kamal Mohila Complex. Ventilated Box mounted (at 1.6m height) in a partly grass-covered ground surface under the shade of a tree, with a direct air corridor from the lake to the point. Approximately 265m distance from the edge of the lake water along the air corridor in North-Eastern direction.		Latitude 23.748209 Longitude 90.375590	Start 8:25a.m. Finish 6:00 p.m.
9	UCILogger8	At the junction between road 9A & 11A, South-West corner of Sultana Kamal Mohila complex. Height 1.6 m from the footpath. 160 m from the edge of the water in North-Western direction.		Latitude 23.747469 Longitude 90.376386	Start 8:45 a.m. Finish 6:00 p.m.

738

739

740

Hatirjheel Lake Urban Stations:

741

742   In the case of Hatirjheel Lake, one urban station UCILogger1 was suspended from the middle of the

743   Mahanagar Bridge above the water of the lake. Urban station UCILogger2 was placed beside the Lake edge.

744   Two Urban stations (UCILogger8 & 3) were placed inside and at the edge of the park beside the lake. The rest

745   of the Urban stations were placed along a road parallel to the prevailing wind direction. All the locations of the

746   urban stations except UCILogger1 could be seen in the Google Earth image of figure 4.

747

748   Figure 17: Location of the Urban stations of field measurement at Hatirjheel Lake on 10 February 2017

749

750   The following table (table 2) provides detailed information about each urban station on each measurement day
751   of the Hatirjheel Lake area.
752
753   Table 2: Data Logger Location at Hatirjheel Lake area,10 February 2017

Sl	Logger Name	Location and Physical Characteristics of location	Location Photo	Geographical Co-ordinate	Duration of the Data Logging
1	UCILogger1	Mahanagar Bridge (Bridge 2). Suspended from the middle of the bridge at 6 m above the top of the water surface		Latitude 23.768043 Longitude 90.413047	Start 8:19 a.m. Finish 5:50 p.m.
2	UCILogger1 - Extech Dual Sensor	Mahanagar Bridge (Bridge 2). Suspended from the middle of the bridge at 6 m above the top of the water surface		Latitude 23.768043 Longitude 90.413047	Start 8:25 a.m. Finish 5:50 p.m.
3	UCILogger2	Opposite of Police Plaza Concord. Cased inside ventilated Particle board box and tied to the branch of a shrub, 1.8 m above a grass-covered ground surface under the shade of a tree, at the edge of the water of Hatirjheel Lake.		Latitude 23.772448 Longitude 90.415489	Start 8:35 a.m. Finish 5:50 p.m.
4	UCILogger2 -Extech Thermo anemometer	Opposite of Police Plaza Concord. Hand Held - 1.2 m above a grass-covered ground surface under the shade of a tree, at the edge of the water of Hatirjheel Lake.		Latitude 23.772448 Longitude 90.415489	Start 8:50 a.m. Finish 5:50 p.m.
5	UCILogger3	Gulshan 1 park, opposite of shooting club. Cased inside ventilated Particle board box and tied to the branch of a shrub, 1.5 m above a partly grass-covered ground surface under the shade of a tree, 190 m (155 m towards east) away from the edge of the water on the southern direction		Latitude 23.774313 Longitude 90.415876	Start 7:50 a.m. Finish 5:50 p.m.
6	UCILogger4	The junction between road 2 & 4. Cased inside ventilated Particle board box and tied to the trunk of a tree, 1.5 m above the paved surface, approximately 425 m (105 m towards NW) away from the edge of the water in the southern direction and 110 m from the lake edge in the western direction.		Latitude 23.776312 Longitude 90.414983	Start 9:06 a.m. Finish 5:50 p.m.

7	UCILogger6	The junction between road 2 & 6. Cased inside ventilated Particle board box and tied to the trunk of the tree, 1.5 m above the paved surface, approximately 550 m (164 m towards NW) away from the edge of the water in the southern direction		Latitude 23.777164 Longitude 90.415349	Start 9:17 a.m. Finish 5:50 p.m.
8	UCILogger7	The junction between road 8 & 2. Cased inside ventilated Particle board box and tied to the trunk of a tree, 1.5 m above the paved surface, approximately 660 m (243 m towards NW) away from the edge of the water in the southern direction		Latitude 23.777975 Longitude 90.415434	Start 9:25 a.m. Finish 5:50 p.m.
9	UCILogger8	Gulshan-1 park, Police Plaza complex corner. Cased inside ventilated Particle board box and tied to the branch of a shrub, 1.5 m above a partly grass-covered ground surface under the shade of a tree, approximately 120 m away from the edge of the water in the southern direction		Latitude 23.773342 Longitude 90.415418	Start 9:45 a.m. Finish 5:50 p.m.
10	UCILogger8 -Davis	Gulshan-1 park, Police Plaza complex corner. 2 m above a partly grass-covered ground surface under the shade of a tree, approximately 120 m away from the edge of the water in the southern direction		Latitude 23.773342 Longitude 90.415418	Start 11:30 a.m. Finish 5:50 p.m.

754

Instruments

756   The instruments used for data collections are EL-USB-2-LCD Temp & RH Data Logger of Lascar
757 Electronics, Extech 445713: Big Digit Indoor/Outdoor Hygro-Thermometer and Extech AN400 Rotating Cup
758 Thermo-Anemometer. All the measurements were done at a pedestrian level in between a height of 1.5 m-2 m.
759 During the first two measurements in both the study areas, the Lascar instruments were Bamboo tripod-mounted
760 in a partly grass-covered ground or paved surface under the shade of a tree. In the second two measurements,
761 Lascar instruments were Ventilated Box mounted under the shade of a tree. In the case of both the wetlands, all
762 the data logging stations were selected on the downwind side of the wetland except one station on Dhanmondi
763 lake, which was chosen on the upwind side.

764

Physiography of the study area

766   The physiography of both the wetlands is the same as they are located on the same physiographic
767 regions and consequent sub regions (Brammer, 2012). The physiographic region of the wetland is Madhupur

768   Tract. Much of the Dhaka city lies on the Madhupur Tract, but in the map (figure 3), it has been shown
769   separately. The other important locational information was that both the lakes were located on the same overall
770   geothermal gradient zone (Akbar, 2011). From the above information it could be safely deduced that in terms
771   of heat gain from the ground source both Dhanmondi and Hatirjheel lakes are in the same category; that means,
772   if they gain heat from the ground, it will be at the same rate. In fact, they will not get any heat at all from the
773   ground source as the geothermal potential in this location is not high enough. So, it is only the differential
774   shading pattern, due to the big riparian shading and the built form, which will create differential solar gain for
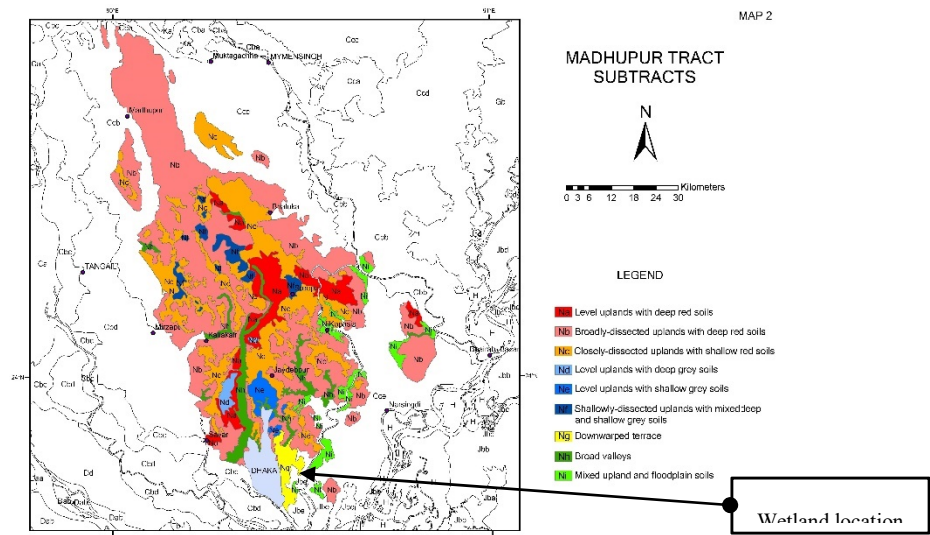775   both the lakes.

776
777   Figure 18: Physiographic region of the wetland area (Brammer, 2012)

778   **Appendix B**

779   **Turbulent Flow:**
780   The flow was modeled using Wilcox k-ω turbulence model. The main reason for using the k-ω model
781   over the k-ε model is that the former is, in general, more reliable when it comes to predicting the spreading rate
782   of jets (Wilcox, 1998). The k-ω model uses wall functions which is appropriate in this case since all walls are
783   almost insulated and there would not be much benefit from using the more expensive low-Re k-ε model.
784   Further, it is assumed that the velocity and pressure field is independent of the air temperature
785   and moisture content. This allows us to calculate the flow field in advance and then use it as input for the
786   heat transfer and species transport equation.

787   **Heat Transfer:**
788   The primary source of heat in this model was the solar irradiation, which was included using the
789   External Radiation Source feature. This feature uses the longitude, latitude, time zone, time of year, and time
790   of day to compute the direction of the incident solar radiation over the simulation time. Assuming no cloud
791   cover, the solar flux at the surface was about 1000 W/m2. "All of the ambient surfaces of the model were
792   included in the solar loading calculation, and shadowing effects were included. The temperature of the sun is
793   about 5800 K, and it emits primarily short-wavelength infrared and visible light at wavelengths shorter than 2.5
794   microns" (COMSOL documentation). The fraction of this short-wavelength solar radiation that is absorbed by
795   the various materials is quantified by the solar absorptivity. Because the surfaces are at a much lower
796   temperature, they reradiate in the long-wavelength infrared band, at wavelengths above 2.5 microns, and the
797   fraction of reradiated energy is quantified by the surface emissivity. "The solar and ambient wavelength

798   dependence of emissivity model was used to account for differing emissivities in different wavelength bands"
799   (COMSOL documentation).

800   The heat transfer between the lake and land is due to conduction only. For the air, convection dominates
801   the heat transfer and the turbulent flow field is required. The material properties were determined by the moist
802   air theory. During evaporation, latent heat was released from the water surface which cools down the water in
803   addition to convective and conductive cooling by the surrounding environment. This means that the fraction of
804   convective and diffusive flux normal to the water surface contributes to the evaporative heat flux (Incropera et
805   al, 2006).

806    $$-n.\,(-k\nabla T) = H_{vap}n.\,(-D\nabla c + uc)$$

807   The latent heat of vaporization H_{vap} is given in kj/mol.

808   **Transport of water vapor:**

809   To obtain the measurement of the correct amount of water evaporated from the lake into the air, the
810   Transport of Diluted Species interface was used in the air domain. The initial concentration was chosen to keep
811   the initial relative humidity (RH) equal to the RH at 9 a.m. in the morning obtained from the field measurement.
812   The source term for water vapor at the water surface is given by the ideal gas law at saturation pressure
813   (Monteith et al, 2013):

814    $$c_{vap} = \frac{p_{sat}}{R_g T}$$

815   The transport equation again uses the turbulent flow field as input. Turbulent has been considered for
816   the diffusion coefficient, by adding the following turbulent diffusivity to the diffusion tensor:

817    $$D_T = \frac{v_T}{Sc_T} I$$

818   Where v_T is the turbulent kinematic viscosity, Sc_T is the turbulent Schmidt number and I the unit matrix.

819

820   **Roughness parameters**

821   Roughness parameters had been specified for five spatial areas inside the computational domain, as
822   suggested by Blocken (2015). Area one is upstream of the computational domain. Area two is the area inside
823   the computational domain and upstream of the explicitly modeled building. Area three inside the computational
824   domain represents the ground surface amidst the explicitly modeled buildings and other obstacles. Area four is
825   the surface of the explicitly modeled buildings (façade, roofs) and structures inside the computational domain.
826   Area five is the area inside the computational domain and downstream of the explicitly modeled buildings.
827   Also, two types of roughness specification had been made (Blocken, 2015):

828   i.   Aerodynamic roughness length z_0: used for area one, two, three and five
829   ii.   Equivalent sand-grain roughness length k_s: used in area four

830   For the Discretization scheme default second-order elements of "COMSOL" are used.

831   **Appendix C**

832   **Reference measurement at Bangladesh Meteorological Department**

833   As stated earlier, one data logger was placed inside the Stevenson screen of the Bangladesh
834   Meteorological department's (BMD) measurement site at Agargaon together with the BMD's instrument. The
835   duration of the measurement was from 11:00 a.m. 12 December 2016 to 11:00 a.m. 14 December 2016. The air

836 temperature and relative humidity data from 6:00 p.m. 12 December to 6:00 a.m. 14 December 2016 of this
837 urban station were analyzed. For the correlational analysis the data was divided into three chunks; first one was
838 6:00 p.m. 12 December to 6:00 a.m. 13 December 2016 (Night); the second one was 6:00 a.m. 13 December to
839 6:00 p.m. 13 December 2016 (Day) and the third one was 6:00 p.m. 13 December to 6:00 a.m. 14 December
840 2016 (Night). Air temperature and relative humidity showed a typical diurnal pattern (Figure 10). At the
841 beginning of the day, air temperature started to rise with a peak between 1:00 p.m. to 3:30 p.m. then started to
842 decline again. Relative Humidity shows the opposite trend, with highest reading at the beginning of the day and
843 continual decline as the day progresses, with the lowest in between 1:00 p.m. to 3:30 p.m. then started to rise
844 again. Air temperature continues to decline after the sunset throughout the night, with the lowest registering
845 between 5:33 a.m. to 7:15 a.m. Again, relative Humidity showed the opposite trend, which continued rising
846 after sunset throughout the night with the highest in between 5:34 a.m. to 7:15 a.m.

847

848
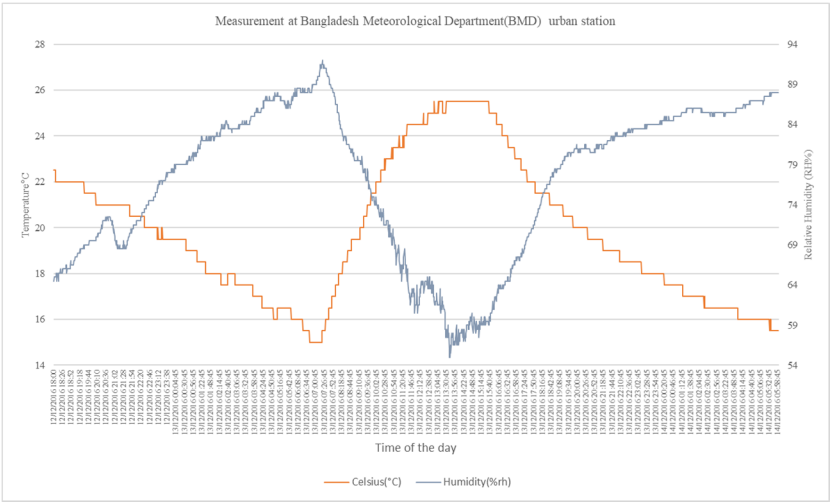
849 Figure 19: Air Temperature and Relative Humidity measurement at Bangladesh Meteorological Urban Station
850 (BMD)

851 Table 3: Correlation coefficient of Air temperature and Relative humidity at the Bangladesh Meteorological
852 Department urban station

Variables	6:00 p.m. 12 December to 6:00 a.m. (Night)	6:00 a.m. 13 December to 6:00 p.m. 13 December 2016 (Day)	6:00 p.m. 13 December to 6:00 a.m. 14 December 2016 (Night)
Air Temperature (Ta)	-0.9917444	0.7866812	-0.9848626
Relative Humidity (RH)	0.9834432	-0.8062279	0.9341942

853

854   The correlation analysis had been done separately by dividing the data into the day (6:00 a.m. to 6:00
855 p.m.) and night (6:00 p.m. to 6:00 a.m.) slots (table 3). At the beginning of the day, the solar influx started to
856 increase as the sun rises which continued till afternoon. After that, solar influx started to decrease towards zero
857 at the sunset. The overall rate of change of solar influx throughout the day is positive. At night, with the absence
858 of sun, there is no solar influx and urban rate of heat loss from the urban fabric is constant till the sunrise.

859

860 **Correlation coefficient between air temperature, Relative Humidity and cumulative**
861 **time of the urban stations at the measurement day:**

862   Table 4: Correlation coefficient between air temperature and cumulative time of the urban stations of
863   Dhanmondi lake on 21 October 2016

Urban stations	correlation coefficient
UCIL1(°C)	0.7287369
UCIL2(°C)	0.3943478
UCIL4(°C)	0.5682237
UCIL6(°C)	0.7629839
UCIL7(°C)	0.06319901

864

865   Table 5: Correlation coefficient between air temperature and cumulative time of the urban stations of
866   Dhanmondi lake on 27 January 2017

urban stations	correlation coefficient
UCIL1(°C)	0.3637763
UCIL2(°C)	-0.7791296
UCIL3(°C)	-0.259729
UCIL4(°C)	0.4463227
UCIL5_Hh(°C)	-0.02484631
UCIL6(°C)	0.4421808
UCIL7(°C)	0.3723458
UCIL8(°C)	-0.7303561
UCIL9_Hh(°C)	0.4710534

867

868

869   Table 6: Correlation coefficient between air temperature and cumulative time of the urban stations of
870   Dhanmondi lake on 24th February 2017

Urban Stations	Distance from the water edge	Correlation coefficient
UCIL1(°C)	0, middle	0.8550726
UCIL2(°C)	0, edge	0.8893085
UCIL3(°C)	80m	0.8769852
UCIL4(°C)	420m	0.873383
UCIL6(°C)	157m	0.7462933
UCIL7(°C)	230m	0.8052079
UCIL8(°C)	206m	0.695779

871

872   Table 7: Correlation coefficient between Relative Humidity and cumulative time of the urban stations of
873   Dhanmondi lake on 21 October 2016

Urban stations	correlation coefficient
UCIL1(%rh)	-0.5848008
UCIL2(%rh)	-0.3303872

UCIL4(%rh)	-0.5752285
UCIL6(%rh)	-0.6392395
UCIL7(%rh)	-0.08758491

874

875   Table 8: Correlation coefficient between Relative Humidity and cumulative time of the urban stations of
876   Dhanmondi lake on 27 January 2017

urban stations	correlation coefficient
UCIL1(%rh)	0.06428339
UCIL2(%rh)	0.7835108
UCIL3(%rh)	0.2770792
UCIL4(%rh)	-0.1739092
UCIL6(%rh)	-0.2526658
UCIL7(%rh)	0.1213577
UCIL8(%rh)	0.6251589

877

878   Table 9: Correlation coefficient between Relative Humidity and cumulative time of the urban stations of
879   Dhanmondi lake on 24th February 2017

Urban Stations	Distance from the water edge	Correlation coefficient
UCIL1(%rh)	0, middle	-0.7073007
UCIL2(%rh)	0, edge	-0.5923311
UCIL3(%rh)	80m	-0.5166587
UCIL4(%rh)	420m	-0.7891712
UCIL6(%rh)	157m	-0.2328342
UCIL7(%rh)	230m	-0.6613266
UCIL8(%rh)	206m	-0.4341711

880

881   Table 10: Correlation coefficient between air temperature and cumulative time of the urban stations of
882   Hatirjheel lake on 11th November 2016

Urban Statins	Distance from the water edge	correlation coefficient
UCIL1(°C)	0m, middle	0.560289187
UCIL2(°C)	190m, park	0.546136277
UCIL6(°C)	0m, edge	0.52784335
UCIL7(°C)	100m	0.386346895
UCIL8(°C)	425m	-0.035748094

883   Table 11: Correlation coefficient between air temperature and cumulative time of the urban stations of
884   Hatirjheel lake on 13th December 2016

Urban stations	correlation coefficient
UCIL1(°C)	0.648584
UCIL2(°C)	0.7980454
UCIL6(°C)	0.9158919
UCIL7(°C)	0.9083694

UCIL8(°C)	0.7867869

885

886   Table 12: Correlation coefficient between air temperature and cumulative time of the urban stations of
887   Hatirjheel lake on 10th February 2017

Urban Stations	Distance from the water edge	correlation coefficient
UCIL1(°C)	0 m	0.9234208
UCIL2(°C)	0 m water Edge	0.8790585
UCIL8(°C)	120 m, middle of the park	0.7683875
UCIL3(°C)	190 m, edge of the park	0.8194174
UCIL4(°C)	425 m	0.5792301
UCIL6(°C)	550 m	0.5944549
UCIL7(°C)	660 m	0.6755592

888

889   Table 13: Correlation coefficient between Relative Humidity and cumulative time of the urban stations of
890   Hatirjheel lake on 11th November 2016

Urban Stations	correlation coefficient
UCIL1(%rh)	-0.4922671
UCIL2(%rh)	-0.5230172
UCIL6(%rh)	-0.4645949
UCIL7(%rh)	-0.3971748
UCIL8(%rh)	-0.1057552

891

892   Table 14: Correlation coefficient between Relative Humidity and cumulative time of the urban stations of
893   Hatirjheel lake on 13th December 2016

Urban stations	correlation coefficient
UCIL1(%rh)	-0.5896493
UCIL2(%rh)	-0.8396173
UCIL6(%rh)	-0.8576293
UCIL7(%rh)	-0.848607
UCIL8(%rh)	-0.8210089

894   Table 15: Correlation coefficient between Relative Humidity and cumulative time of the urban stations of
895   Hatirjheel lake on 10th February 2017

Urban Stations	Distance from the water edge	correlation coefficient
UCIL1(%rh)	0 m	-0.9025281
UCIL2(%rh)	0 m water Edge	-0.9010745
UCIL8(%rh)	120 m, middle of the park	-0.8260548
UCIL3(%rh)	190 m, edge of the park	-0.8866804
UCIL4(%rh)	425 m	-0.7792143
UCIL6(%rh)	550 m	-0.7394349
UCIL7(%rh)	660 m	-0.7949549

896

897 **Correlation coefficient between simulated air temperature, Relative Humidity and**
898 **cumulative time of the urban stations at the measurement day:**

899   Table 16: Case 1 - Correlation analysis of Air Temperature, Relative Humidity and Time

Measurement point	Pearson's product-moment correlation coefficient for air temperature	Pearson's product-moment correlation coefficient for Relative Humidity
UCIL2	0.8956205	0.8866912
UCIL3	0.9110763	0.5179765
UCIL4	0.9209397	-0.8439007
UCIL5	0.9156383	0.6140438
UCIL6	0.8544383	0.1261469
UCIL7	0.9219397	-0.8535848
UCIL8	0.8226153	-0.06217233

900

901   Table 17: Case 2 - Correlation analysis of Air Temperature, Relative Humidity and Time

Measurement point	Pearson's product-moment correlation coefficient for air temperature	Pearson's product-moment correlation coefficient for Relative Humidity
UCIL2	0.9820582	0.734411
UCIL3	0.9386021	0.4670124
UCIL4	0.9383335	-0.8390386
UCIL5	0.9498092	0.5335272
UCIL6	0.8731839	0.1466815
UCIL7	0.9344495	-0.8475209
UCIL8	0.8438288	-0.05475282

902

903   Table 18: Case 3 - Correlation analysis of Air Temperature, Relative Humidity and Time

Measurement point	Pearson's product-moment correlation coefficient for Air Temperature	Pearson's product-moment correlation coefficient for Relative Humidity
UCIL2	0.8161152	0.3497697
UCIL3	0.8424691	-0.3760967
UCIL4	0.9087311	-0.8948763
UCIL5	0.842523	-0.3727366
UCIL6	0.7835263	-0.5478617
UCIL7	0.9143121	-0.8936088
UCIL8	0.7327484	-0.5152106

904

905   Table 19: Case 4 - Correlation analysis of Air Temperature, Relative Humidity and Time

Measurement point	Pearson's product-moment correlation coefficient for Air Temperature	Pearson's product-moment correlation coefficient for Relative Humidity
UCIL2	0.9747011	0.1416486
UCIL3	0.8970227	-0.3672817
UCIL4	0.9285554	-0.8920262
UCIL5	0.912889	-0.3555603
UCIL6	0.8104017	-0.5294822
UCIL7	0.9276761	-0.8903609
UCIL8	0.7581881	-0.4985059

906

907

Table 20: Correlation between inversion height and fetch

	Pearson's product-moment correlation between Inversion height z and fetch x
Case 1	0.8494861
Case 2	0.7983775
Case 3	-0.3815254
Case 4	-0.5927785

908 **Appendix D**

909 **<u>Urban Design Matrix</u>**

910

Figure 20: Urban Design Matrix for Urban wetland

References

1. Ahmed B., Kamruzzaman M., Zhu X., Rahman S.M., and Choi K. (2013). *"Simulating Land Cover Changes and Their Impacts on Land Surface Temperature in Dhaka, Bangladesh." Remote Sens.*, 5, 5969-5998; DOI:10.3390/rs5115969

2. Ahmed K S. 1995. "*Approaches to Bioclimatic Urban Design for the tropics with special reference to Dhaka, Bangladesh*." Ph.D. thesis, Environment and Energy studies Programme, Architectural Association School of Architecture, London.

3. Akbar, M. A. (2011). "*An assessment of the geothermal potential of Bangladesh*." (pp. 1-33, Rep. No. 5). Reykjavik, Iceland: United Nations University.

4. Ahmed, R. (1993). "*In search of the impact of urbanization on the thermal environment of the city of Dhaka, Bangladesh, during the pre-monsoon hot season from 1948 through 1987*". Report of the Technical Conference on Tropical Urban Climates Dhaka, Bangladesh, March 28 - April 2, 1993, World Meteorological Organization (WMO).

5. Bangladesh Bureau of Statistics. (2016) "*Community Report, Dhaka Zila, June 2012*". Population and Housing Census 2011, Statistics and Informatics Division, Ministry of Planning. *Bbsgovbd*. Retrieved March 29, 2016, from http://www.bbs.gov.bd/PageSearchContent.aspx?key=statistical yearbook.

6. Bowler D.E., Mant R., Orr H., Hannah D. M., and Pullin A.S. (2012). "*What are the effects of wooded*

930   *riparian zones on stream temperature*?" Environmental Evidence, 1:3.

931   7.   Brammer, H. (2012). "*The physical geography of Bangladesh*." First edition, The University press limited,
932   Dhaka.

933   8.   Cheng L., Guan D., Zhou L., Zhao Z., Zhou J. (2019). "*Urban cooling island effect of main river on a*
934   *landscape scale in Chongqing, China*." Sustainable Cities and Society, Volume 47, May 2019, 101501.

935   9.   COMSOL   Documentation.   (n.d.).   Retrieved   February   01,   2018,   from
936   https://www.comsol.com/documentation

937   10. Dyer A.J., Crawford T.V. 1965. "*Observations of the microclimate at a leading-edge."* Quarterly Journal
938   of the Royal Meteorological Society **91**: 345–348.

939   11. FAO/ UNDP (1988). "*land resources appraisal of Bangladesh for Agricultural Development Report 2:*
940   *Agro-ecological regions of Bangladesh*". (Rep. No. 2). (1988). FAO.

941   12. Frey C.M., Rigo G., Parlow E. "*Investigation of the daily Urban Cooling Island (UCI) in two coastal cities*
942   *in an arid environment: Dubai and Abu Dhabi (UAE)."* Institute of Meteorology, Climatology and Remote
943   Sensing, Department of Geosciences, University of Basel.

944   13. Fraedrich, K. (1972). "On the evaporation of a lake in warm and dry environment." Tellus, 24: 116–121.
945   DOI:10.1111/j.2153-3490.tb01538.x

946   14. Gupta N., Mathew A., Khandelwal S. (2019) "*Analysis of cooling effect of water bodies on land surface*
947   *temperature in nearby region: A case study of Ahmedabad and Chandigarh cities in India*." The Egyptian
948   Journal of Remote Sensing and Space Sciences 22, 81–93

949   15. Goltz S.M., Pruitt W.O. 1970. "*Spatial and Temporal Variations of Evapotranspiration Downwind from*
950   *the Leading Edge of a Dry Fallow Field."* Div. Technical Report ECOM68-G10-1, Department of Water
951   Science and Engineering, University of California at Davis.

952   16. Han G., Chen H., Yuan L., Cai Y., Han M. (2011). *"Field measurements on micro-climate and cooling*
953   *effect of river wind on urban blocks in Wuhan city."* Multimedia Technology (ICMT), 2011 International
954   Conference on .10.1109/ICMT.2011.6003331

955   17. Huang L., Li J., Zhao D., Zhu J (2008). "*A fieldwork study on the diurnal changes of urban microclimate*
956   *in four types of ground cover and urban heat island of Nanjing, China."* Building and Environment 43, 7–
957   17.

958   18. IPCC. (2014). Climate Change 2014: Synthesis Report. Contribution of Working Groups I, II, and III to
959   the Fifth Assessment Report of the Intergovernmental Panel on Climate Change [Core Writing Team, R.
960   K. Pachauri and L. A. Meyer (eds.)]. IPCC, Geneva, Switzerland, 151 pp.

961   19. Incropera F.P., DeWitt D.P., Bergman T.L., and Lavine A.S. (2006). "*Fundamentals of Heat and Mass*
962   *Transfer,"* 6th ed., John Wiley & Sons.

963   20. Johnson M. F., and Wilby R. L. (2015). "*Seeing the landscape for the trees: Metrics to guide riparian*
964   *shade   management   in   river   catchments*."   Water   Resources   Research,   51,   3754–3769,
965   DOI:10.1002/2014WR016802.

966   21. Kim Y. H., Ryoo, S. B., Baik, J. J., Park, I. S., Koo, H. J., & Nam, J. C. (2008). "*Does the restoration of*
967   *an inner-city stream in Seoul affect local thermal environment"?* Theoretical and applied climatology,
968   92(3-4), 239-248.

969   22. Lang ARG, Evans GN, Ho PY. 1974. "*The influence of local advection on evapotranspiration from*
970   *irrigated rice in a semi-arid region."* Agricultural Meteorology **13**: 5–13.

971   23. Larson L. L. and Larson S. L. (1996). "*Riparian Shade and Stream Temperature: A Perspective*."
972   Rangelands, Vol. 18, No. 4, pp. 149-152.

973   24. Manteghi G., Lamit H.B., and Ossen D.R. (2015). **"***Influence of Street Orientation and Distance to Water
974   Body on Microclimate Temperature Distribution in Tropical Coastal City of Malacca."* International
975   Journal of Applied Environmental Sciences, Volume 10, Number 2, pp. 749-766

976   25. Mitchell V. G., Cleugh H. A., Grimmond C. S. B. and Xu J. (2008) "*Linking urban water balance and
977   energy balance models to analyze urban design options."* Hydrological Processes Hydrol. Process. 22,
978   2891–2900. Published online in Wiley InterScience.

979   26. Missirian, A., Schlenker W. (2017). "*Asylum applications respond to temperature fluctuations."* Science
980   358 (6370), 1610-1614

981   27. Nishimura N., Nomura T., Iyota H. and Kimoto S (1998). "*Novel water facilities for creation of comfortable
982   urban micrometeorology*." Solar Energy Vol. 64, Nos 4–6, pp. 197–207.

983   28. Oke TR. 1979. "*Advectively-assisted evapotranspiration from irrigated urban vegetation."* Boundary-
984   Layer Meteorology **17**: 167–173.

985   29. Oke, T.R., 2006. "*Initial Guidance to Obtain Representative Meteorological Observations at Urban Site."*
986   *World Meteorological Organization, Instruments, and Observing Methods*, IOM Report No. 81,
987   WMO/TD-No. 1250 Available from http://www.wmo.int/web/www/IMOP/publications-IOM-series.html

988   30. Park C.Y., Lee D.K., Asawa T., Murakami A., Kim H.G., Lee M.K., Lee H.S. "*Influence of urban form
989   on the cooling effect of a small urban river*." Landscape and Urban Planning 183 (2019) 26–35.

990   31. Revi A., Satterthwaite D.E., Durand F. A., Morlot J. C., Kiunsi R.B.R., Pelling M., Roberts D.C., and
991   Solecki W., 2014: Urban areas. In: *Climate Change 2014: Impacts, Adaptation, and Vulnerability. Part A:
992   Global and Sectoral Aspects. Contribution of Working Group II to the Fifth Assessment Report of the
993   Intergovernmental Panel on Climate Change*. Cambridge University Press, Cambridge, United Kingdom,
994   and New York, NY, USA, pp. 535-612.

995   32. Rider N.E, Philip J.R., Bradley E.F. (1963). "*The horizontal transport of heat and moisture-a
996   micrometeorological study."* Quarterly Journal of the Royal Meteorological Society **89**: 507–531.

997   33. Rijks DA. 1971. "*Water use by irrigated cotton in Sudan: III. Bowen ratios and advective energy"*. Journal
998   of Applied Ecology **8**: 643–663.

999   34. Robitu M., Musy M., Inard C., Groleau D. (2006) *"Modeling the influence of vegetation and water pond
1000   on urban microclimate."* Solar Energy 80, 435–447.

1001 35. Rutherford J. C., Blackett S., Blackett C., Saito L., Colley R.J.D (1997). "*Predicting the effects of shade
1002   on water temperature in small streams*." New Zealand Journal of Marine and Freshwater Research, 1997,
1003   Vol. 31: 707-721.

1004 36. Rutherford J. C., Marsh N.A., Davies P.M., and Bunn S.E. (2004). "*Effect of patchy shade on stream water
1005   temperature: how quickly do small streams heat and cool*." Marine and freshwater research, 55, 737-748.

1006 37. Saaroni H., Ziv B. (2003). "*The impact of a small lake on heat stress in a Mediterranean urban park: the
1007   case of Tel Aviv, Israel*." Int J Biometeorol 47:156–165 DOI 10.1007/s00484-003-01617

1008 38. Shahjahan ATM and Ahmed K. S. "*Study of urban water bodies in view of potential for micro-climatic
1009   cooling and natural purification of waste water*" in the book " Balanced Urban Development: Options and
1010   Strategies for Liveable Cities." Edited by: Basant Maheshwari, Vijay P. Singh, and Bhadranie Thoradeniya.
1011   Springer International Publishing. The Netherlands. 2016.

1012 39. Shahjahan A.T.M., Ahmed K. S. and Said IB (2018) *"Field Measurement and Simulation of the
1013   Differential Shading of Wetland as Urban Cooling Island in Warm-Humid Environment*." Data in Brief
1014   [submitted].

40. Somers K. A., Bernhardt E.S., Grace J.B., Hassett B. A., Sudduth E.B., Wang S., and Urban DL (2013). *"Streams in the urban heat island: spatial and temporal variability in temperature."* Freshwater Science, 32(1):309–326

41. Steeneveld G.J., Koopmans S., Heusinkveld B.G., Theeuwes N.E. (2014) "*Refreshing the role of open water surfaces on mitigating the maximum urban heat island effect.*" Landscape and Urban Planning 121, 92–96.

42. Sun R., Chen L. (2012). *"How can urban water bodies be designed for climate adaptation?*" Landscape and Urban Planning 105, 27– 33.

43. Sun R., Chen A., Chen L, Lü Y. (2012). *"Cooling effects of wetlands in an urban region: The case of Beijing."* Ecological Indicators 20, 57–64.

44. Sweeney B. W. and Newbold J. D. (2014). "*Streamside forest buffer width needed to protect stream water quality, habitat, and organisms: A literature review.*" Journal of The American Water Resources Association, Vol. 50, No. 3.

45. Taleghani M., Tenpierik M., Dobbelsteen A.V.D., and Sailor DJ (2014) "*Heat in courtyards: A validated and calibrated parametric study of heat mitigation strategies for urban courtyards in the Netherlands.*" Solar Energy 103, 108–124. 2014.

46. Theeuwes N.E., Solcerová A., and Steeneveld G.J. (2013). *"Modeling the influence of open water surfaces on the summertime temperature and thermal comfort in the city."* Journal of Geophysical Research: Atmospheres, 118(16), 8881-8896. DOI:10.1002/jgrd.50704.

47. Tominaga Y., Sato Y. and Sadohara S. (2015) "*CFD simulations of the effect of evaporative cooling from water bodies in a micro-scale urban environment: Validation and application studies.*" Sustainable Cities and Society 19(2015)259–270.

48. United Nations Population Division | Department of Economic and Social Affairs. (n.d.). Retrieved January 30, 2018, from http://www.un.org/en/development/desa/population/index.shtml

49. Wong N.H., Tan C.L., Nindyani A.D.S., Jusuf S.K., and Tan E. (2011). *"Influence of Water bodies on Outdoor Air Temperature in Hot and Humid Climate."* ICSDC, 2011: pp. 81-89. DOI:10.1061/41204(426)11.

50. Xiyan X., Shuming L., Shibo S., Wenwei Z., Ying L., Zhaoming L., Guancheng G., Smith K., Yong C., Wei L., García E.H., Jianning Z.(2019) "*Evaluation of energy saving potential of an urban green space and its water bodies.*" Energy and Buildings, Volumes 188–189, April 1, 2019, Pages 58-70.